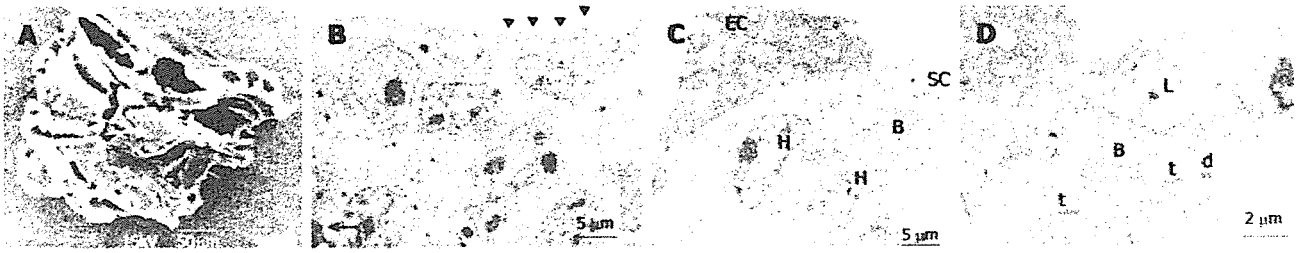

Figure 3 Transmission electron microscopic images of cocultures in the RFB. **A**: The cells are arrayed on the cellulose beads. Several cell clusters could be seen in a gap of cellulose beads (arrow). Vascular lumen structure surrounding cell clusters could be seen in the beads (small arrow). Culture media flow through inside of lumen structure. **B**: The cells are arrayed in layers on cellulose beads. Part of a cellulose bead (arrow) is visible at the bottom of the layer. A process of a sinusoidal endothelial cell (arrowhead) is seen at the perfusion side. Scale bar: 5 μm. **C**: Sinusoidal endothelial cells (EC) can be seen at the perfusion side. Hepatic stellate cells (SC) containing fatty vitamin A droplets are seen overlying the FLC-5 cells (H). FLC-5 cells (H) below EC and SC show bile-canaliculus-like structures (B). Scale bar: 5 μm. **D**: Bile canaliculus-like structures (B) containing electron dense bile components. Tight junctions (t) and desmosomes (d) are visible, as are fatty vitamin A droplets (L). Scale bar: 2 μm.

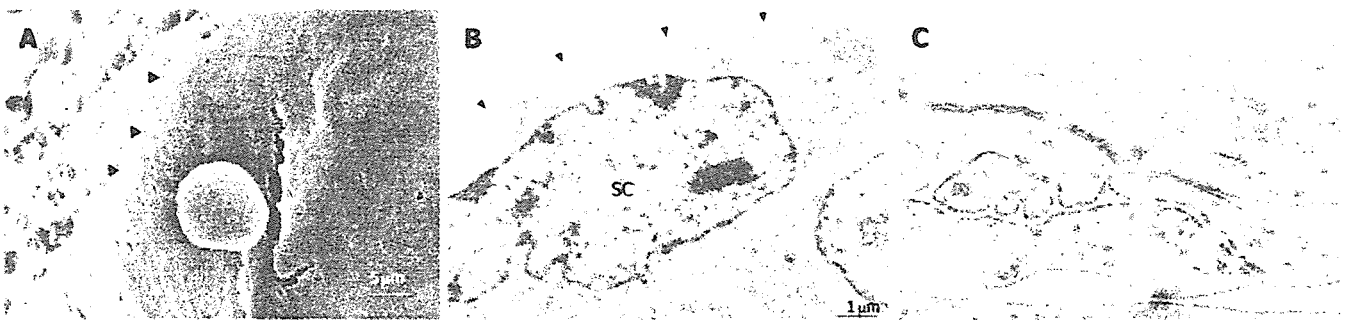

Figure 4 Ultrastructure of sinusoidal endothelial cells. **A**: Scanning electron microscopic image of sinusoidal endothelial cells localized at the perfusion side. They form a thin layer (arrowhead), showing the typical appearance of a sinusoid-like vascular structure. Scale bar: 5 μm. **B**: Transmission electron microscopic image showing sinusoidal endothelial cell growth at the perfusion side forming a thin layer (arrowhead) overlying the A7 cells (SC). Scale bar: 1 μm. **C**: Transmission electron microscopic view showing tight junctions (arrow) between sinusoidal endothelial cells (EC). Scale bar: 200 nm.

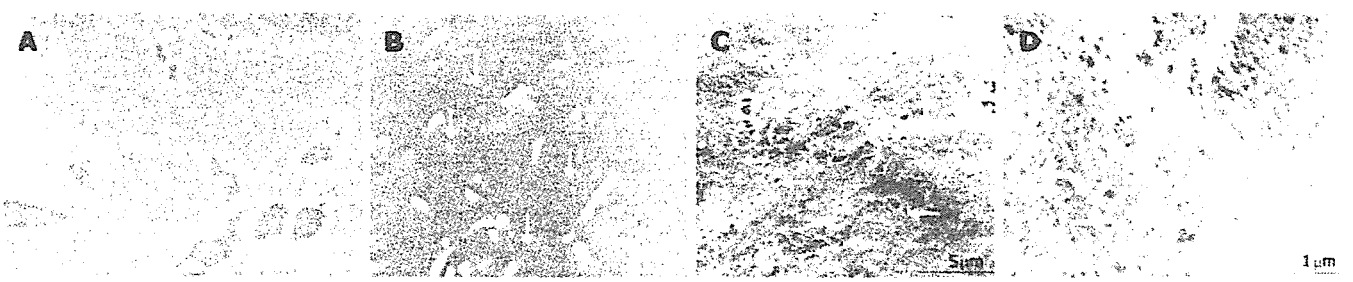

Figure 5 Scanning electron microscopic image of the surface of sinusoidal endothelial cells. **A**: Low-magnification scanning electron microscopic images of the surface of sinusoidal endothelial cells cultured on plastic dishes. The sinusoidal endothelial cells formed a thin layer on the plastic dish substrate. Scale bar: 5 μm. **B**: High-magnification scanning electron microscopy images of the surface of sinusoidal endothelial cells cultured on plastic dishes. Fenestrae could not be detected on the surface of endothelial cells. Only small pits are seen (arrow). Scale bar: 1 μm. **C**: Low-magnification scanning electron microscopic view of the surface of sinusoidal endothelial cells cocultured in the RFB. Fenestrated pores could be observed (arrow). Scale bar: 5 μm; **D**: High-magnification scanning electron microscopic view of the surface of sinusoidal endothelial cells cocultured in the RFB. Pores have a diameter of 100 - 200 nm. Scale bar: 1 μm.

(Figure 3A). TEM showed that cocultured cells assumed layered form from cellulose beads to the perfusion side (Figure 3B). M1 and A7 cells containing vitamin A-laden fat droplets were seen mainly at the perfusion side, while dense layers of FLC-5 cells were observed beneath (Figure 3C). At sites where the three cell lines were in contact with each other bile canaliculus-like structures were present between neighboring FLC-5 cells. Lumens of these structures contained electron-dense bile components, tight junctions and desmosomes also could be observed (Figure 3D). This side showed growth of endothelial cells with the formation of sinusoid-like vascular structures (Figures 4A and 4B). Tight junctions were seen between endothelial cells (Figure 4C). Fenestrae which are characteristic of SEC *in vivo*, were absent in monocultures of M1 cells on plastic dishes (Figures 5A and 5B). Because a long time subculture would change the character of M1 cells, pores were represent on the surface of M1 cells co-cultured in the RFB system (Figure 5C). The pores had a diameter of 100 to 200 nm, being similar in morphology and size to those of fenestrae shown by SEC *in vivo* (Figure 5D).

Morphology of M1 cells incubated with swinholide A

Cells incubated for 2 h with 200 nmol/L of the actin-disrupting agent swinholide A showed the increased number of pores (Figure 6), while some pores were dilated (about

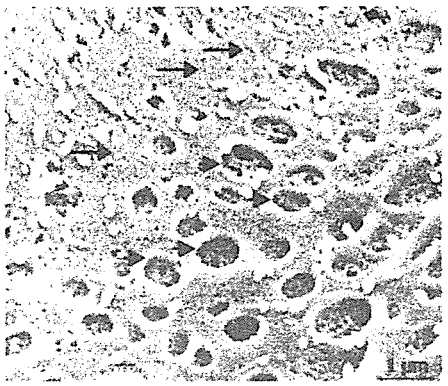

Figure 6 Scanning electron micrographs of the surface of swinholide A - treated SEC cells in the RFB culture system. Large open pores have a fenestra-like appearance (short arrow). Small pores were detectable in the nonfenestrated area (long arrow). Scale bar: 1 μm.

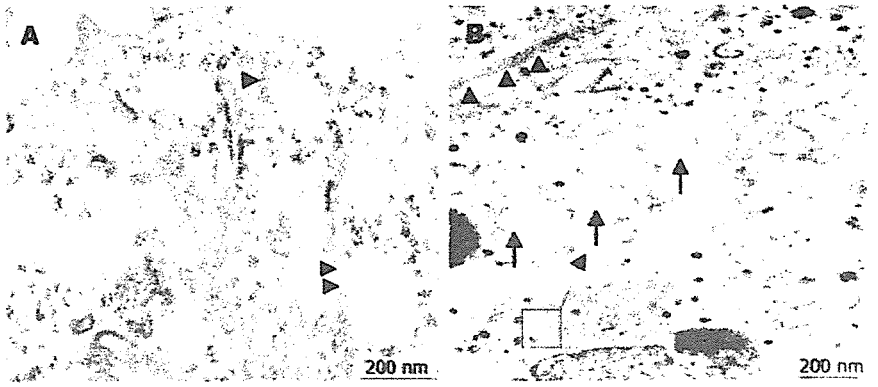

Figure 7 Transmission electron micrographs of sectioned SEC cells after swinholide A - treatment; **A**: Numerous open pores or fenestrae in the cytoplasm (arrow). Fine cytoskeletal elements showing a close spatial relationship with these pores (arrowhead). Scale bar: 200 nm; **B**: VVO could be observed in SEC cells (arrows) in response to stress or actin fibers (arrowheads). Scale bar: 200 nm. Inset shows the overall composition of the cells. Scale bar: 1 μm.

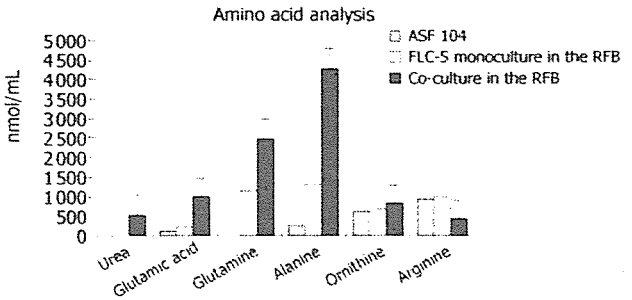

Figure 8 Amino acid and urea analysis in supernatants. Urea was detectable only in coculture, at 523 nmol/ml. ASF 104 designates culture medium. Mean value ± SD.

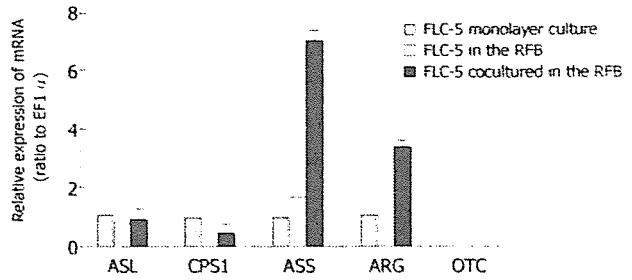

Figure 9 Comparison of expressions of CPS1, OTC, ASS, ASL, and ARG mRNA in FLC-5 incubated under different conditions as assessed by TaqMan 1-step RT-PCR. The mRNA expression of each enzyme in different conditions is relative to that in monolayer cultures. Mean value ± SD.

1 μm). Small pores (tens of nanometers in size) that probably resembled coated pits were abundant in the nonfenestrated areas.

TEM investigation showed that treatment with swinholide A resulted in fenestrated pores with a diameter between 100 and 200 nm. The pores fused with each other formed labyrinthine structures (Figure 7A). In addition, vacuoles with a diameter of about 200 nm, similar to previously described vesiculo vacuolar organelles (VVO), were noted. These structures typically were seen in areas where relatively regular overlap was seen in FLC-5, A7, and M1. The number of VVO increased when cells were treated with 200 nmol/L swinholide A, which was associated with partial fusion (Figure 7B).

Amino acid fractions from supernatants

At the end of culture, the supernatant was subjected to amino acid analysis. Urea production was not seen in monocultures of FLC-5 cells in the RFB, while FLC-5 cells cocultured with M1 and A7 cells produced 523 nmol urea /mL in the culture medium, suggesting that the urea cycle was activated in the coculture RFB system (Figure 8). Several amino acids were increased in the medium.

We compared mRNA expression of CPS1, OTC, ASS, ASL, and ARG in FLC-5 monolayer cultures with those of monocultures in the RFB system. In addition, mRNA expression in cocultures in the RFB also was assessed. We could not detect OTC in any type of culture. Expression of other urea cycle enzymes showed no notable difference between monolayer culture of FLC-5 and monoculture of FLC-5 in the RFB. However, ASS and ARG expressions in co-culture in the RFB were about 7 and 3 times greater than those in FLC-5 monolayer culture (Figure 9).

Albumin synthesis and expression of nuclear factors

We compared mRNA expression of albumin and HNF-1 and HNF-4 as transcription regulation factors between experimental conditions. Expression of mRNA encoding the three proteins was less in FLC-5 co-cultures in the RFB system than in FLC-5 RFB monocultures or in FLC-5 cells in monolayer culture (Figures 10A-10C). In a previous study, albumin production was enhanced in the RFB using the immortalized cell line[19]. However it was different cell line in this study.

DISCUSSION

Introduction of a functional human hepatocellular carcinoma cell line (FLC) in our system can allow the cells to be cultured at high density in a layered array and maintain viability for long periods[18,19].

Immortalized cells can be used for artificial liver. The reason is that it can supply cells in large quantities and quickly. Immortalized cells lose several characteristics in

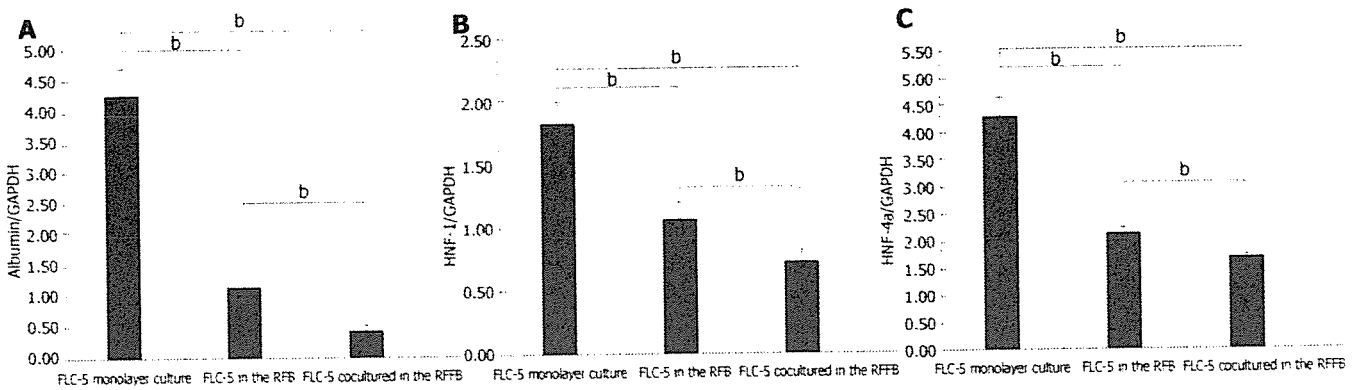

Figure 10 Expression of mRNA for albumin (**A**), HNF-4 (**B**) and HNF-1 (**C**) as transcription regulation factors in each condition. Messenger RNA expression for these three proteins decreased in cocultured FLC-5 in the RFB compared with FLC-5 monocultures in the RFB and FLC-5 cultured in a monolayer. Mean value ± SD. The ratio of mRNA for each protein versus GAPDH is shown. Differences with respect to each condition were statistically significant ($^bP < 0.01$) according to Student's *t*-test.

morphology and function. However, three cell lines were studied in our RFB culture system, including their fine structure according to electron microscopy. Layers of FLC-5, A7, and M1 were arranged respectively from the carrier attachment side to the perfusion side. In some areas, liver-like architectures, sinusoid-like lumen structure, bile-canaliculi and functional complex, were observed, comparable to *in vivo* tissue relationship. The M1 cell line well covered the perfusion side, mimicking vascular structures, indicating that this cell type forms an arrangement similar to that *in vivo*. Furthermore, M1 cells in monolayer culture did not express fenestrae, probably reflecting a long culture or subculture time[20]. In a previous study, we found that M1 cells also lack fenestrae in monocultures in the RFB[19]. In contrasts, fenestrated pores were seen in M1 cells cocultured according to the present RFB experimental design. Coculture and cell to cell contact have an influence on these morphological changes. Because fine structures *in vivo* could be observed better than monoculture in the RFB.

The electron microscopic observations in the present study clearly showed that if an appropriate environment for cell growth was provided in a perfusion culture system, the individual cell types could arrange themselves according to their *in vivo* characteristics, even in a high-density layered culture.

This study also examined the numerical dynamics of fenestrae. For this we exposed the cocultures to the actin-disrupting drug swinholide A[14]. When the cells were treated with swinholide A, the number of pores with a diameter of about 100 to 200 nm increased 2 h after swinholide A treatment. Furthermore, by TEM, cytoplasmic vesicles about 200 nm in diameter could be seen and were much larger than the caveolae in the cytoplasm, and their number increased in the presence of swinholide A. These vacuolar-like vesicles probably represent the vesiculo vacuolar organelle (VVO) as described by Feng *et al*[21]. The VVO is an organelle contributing to transport of macromolecules between luminal and abluminal sides of endothelial cells, thus increasing transcellular permeability. Vascular permeability factor and vascular endothelial growth factor (VPF/VEGF) can induce formation of VVO[22]. FLC-5 used in this study, could express VPF/VEGF (data not shown). The presence of vascular factors may partially explain why VVO is noted in cocultures and why fenestrae could be observed in our experiments[22]. VVO is thought to be formed by fusion of caveolae, when multiple VVOs fuse together, a structure extending from the luminal to the abluminal sides of endothelial cells is formed. In the present study, fused VVOs also were seen in swinholide A - treated specimens by transmission electron microscopy, suggesting that this fusion represents a process culminating in formation of the labyrinthine structures in SEC[24]. The mechanism of pore formation in immortalized SEC and under cocultured perfusion conditions remains unknown from the present study. However, pore formation may result from multiple effects or factors working in concert upon endothelial cells, such as cytoskeletal dynamics represented by actin and/or the influence of a yet unknown factor secreted by other cell types present in the cocultures such as VEGF. The observation that hepatic endothelial cells maintain one of their typical morphological features (i.e. an abundant number of membrane-bound coated-pits, uncoated vesicles/vacuoles and fenestrae) is an indication that the bioreactor mimics a nearby physiological cultivation environment for the various liver cell types. However, the mechanism by which the bioreactor and its culture environment bring about and maintain these membrane-bound vesicles and fenestrae in endothelial cells remain to be elucidated and consequently open up new directions for future experiments.

To assess hepatocyte function, we compared mRNA expression for urea cycle enzymes and albumin synthesis by FLC-5 in monolayer culture compared to these single-type cultures and cocultures in the RFB. Previously, we have demonstrated hepatocyte functions such as albumin synthesis and cytochrome expression are enhanced in the RFB[25, 26]. Urea production is among the most primitive functions of liver cells. We could not detect urea in medium from monolayer cultures or monocultured FLC-5 in the RFB. In contrast, FLC-5 cells cocultured in the RFB exhibit ability to produce urea, and mRNA expression for ASS and ARG is enhanced. The medium used in this experiment, ASF 104 contained arginine, so urea production was observed in cocultures in the RFB although OTC was not expressed. One report showed that urea produc-

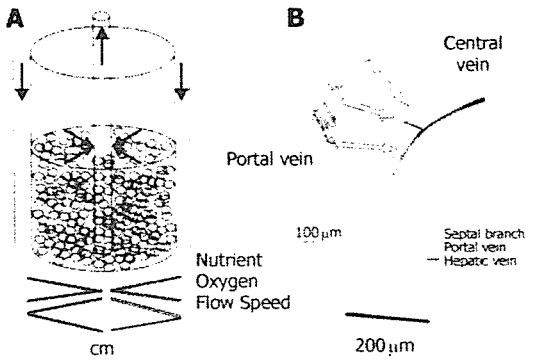

Figure 11 RFB and intact organ. **A**: In the RFB system, culture medium flows from outside the column toward the center of the reactor. Medium flows faster at the center than at the periphery. Biases in distribution of oxygen and nutrition at inflow and outflow are minimized. **B**: In the hepatic lobe, blood flows from the portal vein to central vein. The RFB system is similar to the organization of the hepatic primary lobe[31]. Figure 11B is reproduced from Figure 9 in reference 31.

tion in OTC-deficient mice could be detected under the same condition[27]. Glutamic acid, glutamine and alanine were also increased in supernatant co-cultured in the RFB, indicating that amino acid metabolism becomes active.

It was reported that three-dimensional spherical culture induces albumin synthesis, a particularly important hepatocytic function[28, 29]. However, in the present study, mRNA expression of albumin was decreased under co-culture conditions in the RFB. Nuclear transcriptional factors HNF-4 and HNF-1, which regulate albumin synthesis, were decreased under coculture conditions in the RFB. Albumin in supernatant was also decreased during culture (data not shown). The results suggest that the culture environment (cell-to-cell communication, cell polarity, shear stress, and other factors) can control manifestations of intracellular nuclear transcription factors and therefore dramatically influence albumin production by liver cells. Immortalized cells can be used for artificial liver. The reason is that it can supply cells in large quantities and quickly. But immortalized cells may change the characteristics of its original cells. In this study, albumin synthesis was decreased. It was not useful for artificial liver. In future study, we have to try other cell sources (ES cell, oval cell, and other immortalized cell lines).

Finally, several points should be noted concerning our culture system. First, controlling the mixture ratio of the three cell types used is very difficult since each type possesses its own potential for active growth. Thus, growth rates vary between cell types and are difficult to control. For examples, A^- cells grew less rapidly and tended to be less than the other two cell types in the coculture system. Second, the hepatic lobule spans about 140 μm *in vivo*, extending from the portal to the central area, toward which portal blood flows in a radial manner. According to Matsumoto *et al*[30], the liver is an organ composed of numerous groups of microscopic three-dimensional units (minimal radial-flow bioreactors) extending from the inflow side (composed of combinations of parabola-shaped inflow fronts) to the central vein[31]. According to this model, the liver microcirculation as observed *in vivo* could not be reproduced faithfully with a radial-flow bioreactor, since the distance between inflow and outflow sides in the bioreactor is about 1.5 cm (Figure 11). Third, bile canaliculus-like structures are formed between hepatocytes. Since we did not use the bile duct cells in this study, whether different cell types can reconstruct bile ducts remains to be elucidated[32]. Finally, although several questions remain, the results of the present study suggest that liver reconstruction is possible *in vitro*. Such organ reconstruction technology is expected to contribute greatly to the development of sophisticated artificial livers and other organs for transplantation. Our culture system may be a very important tool to maintain liver organ.

ACKNOWLEDGMENTS

The authors thank Mr. Hideki Saito, Mrs. Emi Kikuchi, and Mrs. Hisako Arai of the DNA Medical Institute at The Jikei University School of Medicine for technical assistance with electron microscopy. The authors also thank the members of the Australian Key Center for Microscopy and Microanalysis of The University of Sydney for their excellent administrative, technical, and practical support.

REFERENCES

1 **Gordon GJ,** Butz GM, Grisham JW, Coleman WB. Isolation, short-term culture, and transplantation of small hepatocyte-like progenitor cells from retrorsine-exposed rats. *Transplantation* 2002; **73**: 1236-1243

2 **Kanda T,** Watanabe S, Yoshiike K. Immortalization of primary rat cells by human papillomavirus type 16 subgenomic DNA fragments controlled by the SV40 promoter. *Virology* 1988; **165**: 321-325

3 **Nishida K,** Yamato M, Hayashida Y, Watanabe K, Yamamoto K, Adachi E, Nagai S, Kikuchi A, Maeda N, Watanabe H, Okano T, Tano Y. Corneal reconstruction with tissue-engineered cell sheets composed of autologous oral mucosal epithelium. *N Engl J Med* 2004; **351**: 1187-1196

4 **Nishida K,** Yamamoto M, Hayashida Y. Corneal reconstruction using tissue-engineered cell sheets comprising autologous oral mucosal epithelium. *N Engl J Med* 2004; **351**: 1187-1196

5 **Tabata Y.** Tissue regeneration based on growth factor release. *Tissue Eng* 2003; **9 Suppl 1**: S5-S15

6 **Sussman NL,** Chong MG, Koussayer T, He DE, Shang TA, Whisennand HH, Kelly JH. Reversal of fulminant hepatic failure using an extracorporeal liver assist device. *Hepatology* 1992; **16**: 60-65

7 **Sussman NL,** Kelly JH. Improved liver function following treatment with an extracorporeal liver assist device. *Artif Organs* 1993; **17**: 27-30

8 **Matsuura T,** Kawada M, Hasumura S, Nagamori S, Obata T, Yamaguchi M, Hataba Y, Tanaka H, Shimizu H, Unemura Y, Nonaka K, Iwaki T, Kojima S, Aizaki H, Mizutani S, Ikenaga H. High density culture of immortalized liver endothelial cells in the radial-flow bioreactor in the development of an artificial liver. *Int J Artif Organs* 1998; **21**: 229-234

9 **Matsuura T,** Kawada M, Sujino H, Hasumura S, Nagamori S, Shimizu H. Vitamin A metabolism of immortalized hepatic stellate cell in the bioreactor. In: Wisse E, Knook D L, De Zanger R, Arthur M J P, eds. Cells of the Hepatic Sinusoid 7. Leiden: *Kupffer Cell Foundation*, 1999; 88-89

10 **Jat PS,** Noble MD, Ataliotis P, Tanaka Y, Yannoutsos N, Larsen L, Kioussis D. Direct derivation of conditionally immortal cell lines from an H-2Kb-tsA58 transgenic mouse. *Proc Natl Acad Sci USA* 1991; **88**: 5096-5100

11 **Wisse E.** An electron microscopic study of the fenestrated endothelial lining of rat liver sinusoids. *J Ultrastruct Res* 1970; **31**:

125-150
12 **Braet F.** How molecular microscopy revealed new insights into the dynamics of hepatic endothelial fenestrae in the past decade. *Liver Int* 2004; **24**: 532-539
13 **Fraser R**, Dobbs BR, Rogers GW. Lipoproteins and the liver sieve: the role of the fenestrated sinusoidal endothelium in lipoprotein metabolism, atherosclerosis, and cirrhosis. *Hepatology* 1995; **21**: 863-874
14 **Braet F**, Spector I, De Zanger R, Wisse E. A novel structure involved in the formation of liver endothelial cell fenestrae revealed by using the actin inhibitor misakinolide. *Proc Natl Acad Sci USA* 1998; **95**: 13635-13640
15 **Braet F**, Spector I, Shochet N, Crews P, Higa T, Menu E, de Zanger R, Wisse E. The new anti-actin agent dihydrohalichondramide reveals fenestrae-forming centers in hepatic endothelial cells. *BMC Cell Biol* 2002; **3**: 7
16 **Oda M**, Tsukada N, Komatsu H, Kaneko K, Nakamura M, Tsuchiya M: Electron microscopic localizations of actin, calmodulin and calcium in the hepatic sinusoidal endothelium in the rat. In: Kirn A, Knook DL, Wisse E des. Cells of the Hepatic Sinusoid 1. Rijswijk, *Kupffer Cell Foundation* 1986, 511-512
17 **Gatmaitan Z**, Varticovski L, Ling L, Mikkelsen R, Steffan AM, Arias IM. Studies on fenestral contraction in rat liver endothelial cells in culture. *Am J Pathol* 1996; **148**: 2027-2041
18 **Kawada M**, Nagamori S, Aizaki H, Fukaya K, Niiya M, Matsuura T, Sujino H, Hasumura S, Yashida H, Mizutani S, Ikenaga H. Massive culture of human liver cancer cells in a newly developed radial flow bioreactor system: ultrafine structure of functionally enhanced hepatocarcinoma cell lines. *In Vitro Cell Dev Biol Anim* 1998; **34**: 109-115
19 **Aizaki H**, Nagamori S, Matsuda M, Kawakami H, Hashimoto O, Ishiko H, Kawada M, Matsuura T, Hasumura S, Matsuura Y, Suzuki T, Miyamura T. Production and release of infectious hepatitis C virus from human liver cell cultures in the three-dimensional radial-flow bioreactor. *Virology* 2003; **314**: 16-25
20 **Braet F**, de Zanger R, Seynaeve C, Baekeland M, Wisse E. A comparative atomic force microscopy study on living skin fibroblasts and liver endothelial cells. *J Electron Microsc (Tokyo)* 2001; **50**: 283-290
21 **Feng D**, Nagy JA, Hipp J, Dvorak HF, Dvorak AM. Vesiculovacuolar organelles and the regulation of venule permeability to macromolecules by vascular permeability factor, histamine, and serotonin. *J Exp Med* 1996; **183**: 1981-1986
22 **Feng D**, Nagy JA, Pyne K, Hammel I, Dvorak HF, Dvorak AM. Pathways of macromolecular extravasation across microvascular endothelium in response to VPF/VEGF and other vasoactive mediators. *Microcirculation* 1999; **6**: 23-44
23 **Yokomori H**, Oda M, Yoshimura K, Nagai T, Ogi M, Nomura M, Ishii H. Vascular endothelial growth factor increases fenestral permeability in hepatic sinusoidal endothelial cells. *Liver Int* 2003; **23**: 467-475
24 **Oda M**, Yokomori H, Han J Y, Kamegaya Y, Ogi M, Nakamura M. Hepatic sinusoidal endothelial fenestrae are a stationary type of fused and interconnected caveolae. In: Wisse E, Knook D L, De Zanger R, Arthur M J P, eds. Cells of the Hepatic Sinusoid 8. Leiden: *Kupffer Cell Foundation*, 2001: 94-98
25 **Nagamori S**, Hasumura S, Matsuura T, Aizaki H, Kawada M. Developments in bioartificial liver research: concepts, performance, and applications. *J Gastroenterol* 2000; **35**: 493-503
26 **Iwahori T**, Matsuura T, Machashi H, Sugo K, Saito M, Hosokawa M, Chiba K, Masaki T, Aizaki H, Ohkawa K, Suzuki T. CYP3A4 inducible model for in vitro analysis of human drug metabolism using a bioartificial liver. *Hepatology* 2003; **37**: 665-673
27 **Li MX**, Nakajima T, Fukushige T, Kobayashi K, Seiler N, Saheki T. Aberrations of ammonia metabolism in ornithine carbamoyltransferase-deficient spf-ash mice and their prevention by treatment with urea cycle intermediate amino acids and an ornithine aminotransferase inactivator. *Biochim Biophys Acta* 1999; **1455**: 1-11
28 **Glicklis R**, Merchuk JC, Cohen S. Modeling mass transfer in hepatocyte spheroids via cell viability, spheroid size, and hepatocellular functions. *Biotechnol Bioeng* 2004; **86**: 672-680
29 **Ma M**, Xu J, Purcell WM. Biochemical and functional changes of rat liver spheroids during spheroid formation and maintenance in culture: I. morphological maturation and kinetic changes of energy metabolism, albumin synthesis, and activities of some enzymes. *J Cell Biochem* 2003; **90**: 1166-1175
30 **MacSween R**. N. M. Pathology of the Liver, 4th ed. In: Developmental anatomy and normal structure, *Churchill Livingstone*, 2002: 16-22
31 **Matsumoto T**, Komori R, Magara T, Ui T, Kawakami M, Hano H. A study on the normal structure of the human liver, with special reference to its angioarchitecture. *Jikei Med J* 1979; **26**: 1-40
32 **Ishida Y**, Smith S, Wallace L, Sadamoto T, Okamoto M, Auth M, Strazzabosco M, Fabris L, Medina J, Prieto J, Strain A, Neuberger J, Joplin R. Ductular morphogenesis and functional polarization of normal human biliary epithelial cells in three-dimensional culture. *J Hepatol* 2001; **35**: 2-9

S- Editor Wang J **L- Editor** Wang XL **E- Editor** Liu WF

All-*trans* retinoic acid down-regulates human albumin gene expression through the induction of C/EBPβ-LIP

Takahiro MASAKI*†‡, Tomokazu MATSUURA§, Kiyoshi OHKAWA†, Tatsuo MIYAMURA*, Isao OKAZAKI‡, Tetsu WATANABE‡ and Tetsuro SUZUKI*[1]

*Department of Virology II, National Institute of Infectious Diseases, Tokyo 162-8640, Japan, †Department of Biochemistry, The Jikei University School of Medicine, Tokyo 105-8461, Japan, ‡Department of Community Health, Tokai University School of Medicine, Kanagawa 259-1193, Japan, and §Department of Laboratory Medicine, The Jikei University School of Medicine, Tokyo 105-8461, Japan

ATRA (all-*trans* retinoic acid), which is a major bioactive metabolite of vitamin A and a potent regulator of development and differentiation, mediates down-regulation of the human albumin gene. However, the mechanism of ATRA-mediated down-regulation is not well understood. In the present study, deletion analysis and luciferase assays demonstrate that ATRA causes a marked decrease in the activity of the albumin promoter, the region between nt -367 and -167 from the transcription start site, where C/EBP (CCAAT/enhancer-binding protein)-binding sites are tightly packed, is indispensable for ATRA-mediated down-regulation. ChIP (chromatin immunoprecipitation) assays revealed that *in vivo* binding of C/EBPα to the region markedly decreases upon incubation with ATRA, whereas ATRA treatment marginally increases the recruitment of C/EBPβ. We found that ATRA has the ability to differentially and directly induce expression of a truncated isoform of C/EBPβ, which is an LIP (liver-enriched transcriptional inhibitory protein) that lacks a transactivation domain, and to increase the binding activity of C/EBPβ-LIP to its response element. Overexpression of C/EBPβ-LIP negatively regulates the endogenous expression of albumin, as well as the activity of the albumin promoter induced by C/EBP transactivators such as C/EBPα and full-length C/EBPβ. In conclusion, we propose a novel model for down-regulation of the albumin gene, in which ATRA triggers an increase in the translation of C/EBPβ-LIP that antagonizes C/EBP transactivators by interacting with their binding sites in the albumin promoter.

Key words: all-*trans* retinoic acid (ATRA), liver-enriched transcription factor, CCAAT/enhancer-binding protein (C/EBP), dominant-negative factor, FLC-4 cell, liver-enriched transcriptional inhibitory protein (LIP).

INTRODUCTION

Serum albumin is the most abundant and characteristic protein that is produced by the mature liver; albumin functions as a transporter of various substances and is a prime regulator of colloid osmotic pressure [1]. Albumin is exclusively synthesized in the liver, approx. 200 mg/kg per day [2], leading to its high steady-state concentration in plasma (35–50 g/l in humans). It has been reported that the albumin level in plasma is decreased as a result of reduced albumin synthesis in clinical disorders such as liver disease [2], infectious disease [3], and cancer [4]. Serum albumin can be used as a reliable indicator for the prognosis and severity of these diseases [5,6]. Therefore it is probable that albumin synthesis is regulated accurately and dramatically in a variety of physiological and pathophysiological conditions.

Albumin synthesis is regulated mainly at the transcriptional level through tissue-specific transcription factors such as HNF (hepatocyte nuclear factor)-1 and C/EBP (CCAAT/enhancer-binding protein) [7,8]. The transcription of the albumin gene is down-regulated by a number of factors, including cytokines [9–11], vitamins [12–14], colloid osmotic pressure [15,16] and amino acid limitation [17]. ATRA (all-*trans* retinoic acid), a major bioactive metabolite of vitamin A, plays a crucial role in hepatocyte differentiation, proliferation and apoptosis [18,19]. ATRA has been shown to down-regulate albumin gene expression in rat hepatocytes [20] and human hepatoma cell lines [12,13]. In animal experiments, it has been reported that a decrease in serum albumin concentration is observed after the administration of ATRA to rodents [21]. Furthermore, in clinical studies of fenretinide (4-hydroxyphenyl-retinamide), a synthetic derivative of ATRA that posesses inhibitory activity against various types of malignant cells [22–24], administration of the drug caused hypoalbuminemia as an adverse effect [25]. Nevertheless, little is known about the ATRA-mediated down-regulation of albumin expression either in experimental or clinical research fields.

In the present study, we have examined the molecular mechanism by which ATRA down-regulates albumin expression in human HCC (hepatocellular carcinoma) cells, with special attention to the transcription factors involved. We present evidence that ATRA preferentially induces the expression of a truncated isoform of C/EBPβ: 20 kDa LIP (liver-enriched transcriptional inhibitory protein). We also present evidence that C/EBPβ-LIP functions as an antagonist of C/EBP transactivators in the expression of the albumin gene.

EXPERIMENTAL

Plasmids

The promoter fragment of the human albumin gene between nt -1867 and $+39$ was obtained by PCR amplification using the genomic DNA of human HCC FLC-4 cells [26,27] as a

Abbreviations used: ATRA, all-*trans* retinoic acid; C/EBP, CCAAT/enhancer-binding protein; C/EBPβ-FL, C/EBPβ-full-length; ChIP, chromatin immunoprecipitation; CUG-BP1, CUG triplet-repeat binding protein 1; DR, direct repeat; eIF, eukaryotic translation initiation factor; EMSA, electrophoretic mobility-shift assay; HCC, hepatocellular carcinoma; HNF, hepatocyte nuclear factor; LAP, liver-enriched transcriptional activator protein; LIP, liver-enriched transcriptional inhibitory protein; RARE, retinoic acid response element; RT, reverse transcriptase.

[1] To whom correspondence should be addressed (email tesuzuki@nih.go.jp).

template; the forward primer (5′-GGCTAGCCTGGACTAATATTATTCTTTTCATTTG-3′) and the reverse primer (5′-CCTCGAGGTGTGCCAAAGGCGTGTGGGGTT-3′) contain restriction sites for NheI and XhoI respectively at the 5′ end. After PCR amplification, the 1.9 kb product was digested with NheI and XhoI and it was then ligated into the pGL3-Basic vector (Promega, Madison, WI, U.S.A.) to produce pAL1.9-LUC. A series of human albumin promoter 5′end-deletion constructs were created by PCR amplification using the above reverse primer and the following forward primers: 1456 bp construct (nt −1417 to +39), 5′-GGCTAGCCAGTACCCATTTCTGAAGAAG-3′; 806 bp construct (nt −767 to +39), 5′-GGCTAGCCCTCATTTGGGTCCATTTTCC-3′; 606 bp construct (nt −567 to +39), 5′-GGCTAGCCAGCTTTTTCAGACAGAATGG-3′; 406 bp construct (nt −367 to +39), 5′-GGCTAGCCTATTTAGTTTGGTTAGTAAT-3′ and 206 bp construct (nt −167 to +39), 5′-GGCTAGCCCAGATGGTAAATATACACAA-3′. Each NheI/XhoI fragment was inserted into the pGL3-Basic vector, to yield pAL1.4-LUC, pAL0.8-LUC, pAL0.6-LUC, pAL0.4-LUC or pAL0.2-LUC. To create expression plasmids for C/EBPα, C/EBPβ-FL (C/EBPβ-full-length) and C/EBPβ-LIP, the corresponding sequences were amplified by PCR using pCMV-C/EBPα and pCMV-C/EBPβ, which were provided by Dr G. J. Darlington (Department of Pathology, Baylor College of Medicine, Houston, TX, U.S.A.), as templates and primers containing an EcoRI site at the 5′ ends. Each EcoRI fragment was cloned into the EcoRI site of the pCAGGS vector [28].

Cell culture and treatment with ATRA

FLC-4 cells were maintained in ASF104 serum-free medium (Ajinomoto, Tokyo, Japan) without any supplements, at 37 °C in a humidified 5 % CO_2/95 % air atmosphere. In experiments using ATRA, FLC-4 cells were cultured in ASF104 serum-free medium with or without 1–1000 nmol/l ATRA (Sigma, St. Louis, MO, U.S.A.). For transient transfection experiments, FLC-4 cells were cultured in Dulbecco's modified Eagle's medium supplemented with 100 units/ml penicillin, 100 μg/ml streptomycin and 10 % foetal bovine serum.

ELISA

Albumin levels in culture medium were measured using a human albumin ELISA quantification kit (Bethyl Laboratories, Montgomery, TX, U.S.A.) according to the manufacturer's instructions.

RNA isolation and real-time RT (reverse transcriptase)-PCR

Total RNA was extracted from FLC-4 cells using the RNeasy mini kit (QIAGEN, Tokyo, Japan) according to the manufacture's protocol. Quantitative real-time RT-PCR analysis was performed using the ABI Prism 7700 Sequence Detector (PerkinElmer Applied Biosystems, Foster City, CA, U.S.A.) as described previously [29]. The standard curve was created using serially diluted total RNA obtained from FLC-4 cultures. The amount of target gene expression was calculated from the standard curve, and its quantitative normalization in each sample was carried out using β-actin (PerkinElmer Applied Biosystems) as an internal control. The following primers and fluorescent dual-labelled probes were used: albumin forward primer, 5′-CGATTTTCTTTTTAGGGCAGTAGC-3′; albumin reverse primer, 5′-TGGAAACTTCTGCAAACTCAGC-3′; albumin probe, 5′-CGCCTGAGCCAGAGATTTCCCA-3′; HNF-1α forward primer, 5′-AGCGGGAGGTGGTCGATAC-3′; HNF-1α reverse primer, 5′-CATGGGAGTGCCCTTGTTG-3′; HNF-1α probe, 5′-TCAACCAGTCCCACCTGTCCCAACA-3′; HNF-1β forward primer, 5′-AGCCCAGTTTCCCTTCTATGC-3′; HNF-1β reverse primer, 5′-TCCTCTTCGGTGGTTCCTTGT-3′; HNF-1β probe, 5′-CACAATGCCTCTCCCACGATGTCAAG-3′; C/EBPα forward primer, 5′-CAACGTGGAGACGCAGCA-3′; C/EBPα reverse primer, 5′-GCTCAGCTGTTCCACCCG-3′; C/EBPα probe, 5′-CTGACCAGTGACAATGACCGCCTGC-3′; C/EBPβ forward primer, 5′-GCCCTCGCAGGTCAAGAG-3′; C/EBPβ reverse primer, 5′-TGCGCACGGCGATGT-3′ and C/EBPβ probe, 5′-CAAGCACAGCGACGAGTACAAGATCCG-3′.

Plasmid transfection and luciferase assay

For the expression of luciferase reporter plasmids in FLC-4 cells, 1×10^5 cells per 22 mm well were seeded and cultured overnight. The adherent cells were transfected with 5 μg of plasmid DNA using TransIT-LT1 transfection reagent (Mirus, Madison, WI, U.S.A.) according to the manufacturer's instructions. After the transfection, the cells were incubated with the fresh medium in the presence or absence of 100 nmol/l ATRA for 48 h, followed by determination of the luciferase activity in cells by using the Dual-Luciferase Reporter Assay System (Promega) according to the manufacturer's instructions. For co-expression with C/EBPs, FLC-4 cells were seeded at 2×10^5 cells per 22 mm well on the day before transfection. The cells were transfected with C/EBP expression vectors and the luciferase reporter, pAL1.9-LUC, using TransIT-LT1 transfection reagent, and were cultured for an additional 48 h before the luciferase assay. The total amount of transfected DNA was kept constant by the addition of an empty vector. The pRL-CMV vector (Promega) was used as an internal control for the luciferase assay. To examine the effect of C/EBPs on endogenous albumin expression, FLC-4 cells were seeded at 2×10^5 cells per 22 mm well and cultured overnight. The adherent cells were transfected with C/EBP expression vectors and/or an empty vector using TransIT-LT1 transfection reagent. One day later, the culture medium was changed and the cells were incubated for a further 48 h. After harvesting the medium, the amount of secreted albumin was measured by ELISA.

Western blotting

The proteins were transferred on to a PVDF membrane (Immobilon; Millipore, Bedford, MA, U.S.A.) after separation by SDS/PAGE (12.5 or 15 % gels). After blocking, the membrane was probed with a rabbit polyclonal anti-C/EBPα antibody (sc-61; Santa Cruz Biotechnology, Santa Cruz, CA, U.S.A.), a rabbit polyclonal anti-C/EBPβ antibody (sc-150; Santa Cruz Biotechnology), or a mouse monoclonal anti-β-actin antibody (Sigma), followed by incubation with a peroxidase-conjugated secondary antibody and visualization with a SuperSignal West Pico Chemiluminescent Substrate (Pierce Biotechnology, Rockford, IL, U.S.A.). The amount of protein signal was quantified by densitometric analysis (Cool Saver AE-6955; ATTO, Tokyo, Japan).

ChIP (chromatin immunoprecipitation) assay

ChIP assays were performed using the protocol for the ChIP assay kit (Upstate, Lake Placid, NY, U.S.A.). Briefly, FLC-4 cells in 100 mm dishes were grown to 70 % confluency with or without ATRA treatment for 48 h. The chromatin from formaldehyde-fixed FLC-4 cells was sonicated and immunoprecipitated using the rabbit polyclonal anti-C/EBPα or anti-C/EBPβ antibodies. The chromatin immunoprecipitate was analysed by PCR (33 cycles) with the following primer pairs (F1/R1 and F2/R2) for two different regions of the albumin gene: the region from nt −414

to −188 containing four potential binding sites for C/EBP, F1 (5′-GCAATTTGGGACTTAACTCTTTCAGTA-3′) and R1 (5′-CCTTGTCAATGTATTAAAGTTGTGTAAAACA-3′); and the region from nt −876 to −638 without binding sites for C/EBP, F2 (5′-CAGGGATGGAAAGAATCCTATGCC-3′) and R2 (5′-CCATGTTCCCATTCCTGCTGT-3′).

EMSA (electrophoretic mobility-shift assay)

Nuclear proteins were extracted from FLC-4 cells that were treated with or without 100 nmol/l ATRA for 48 h, or that transiently expressed the LIP protein, using NE-PER Nuclear and Cytoplasmic Extraction reagents (Pierce Biotechnology). A LightShift Chemiluminescent EMSA kit (Pierce Biotechnology) was used to verify the DNA binding of C/EBPβ-LIP to potential C/EBP-responsive sequences in the region from nt −414 to −188 of the albumin gene. Nuclear protein (4 μg) was incubated with the double-stranded biotinylated oligonucleotide that contained the C/EBP-binding site (5′-GTAAAATTTGATAAGATGTT-3′) for 20 min at room temperature. For competition or supershift assay, a 50-fold molar excess of unlabelled wild-type or mutant oligonucleotides (5′-GTAAAAACTGATACAATGTT-3′), or 1 μg of the monoclonal anti-C/EBPβ antibody (sc-7962 X; Santa Cruz Biotechnology) was incubated with nuclear extracts for 30 min before the addition of labelled oligonucleotides. Reaction mixtures were then separated on a 6% native polyacrylamide gel, and shifted bands that corresponded to protein–DNA complexes were captured by a horse radish peroxidase-based detection system.

Statistical analysis

Student's t test was used to evaluate the statistical difference between groups. All P values were obtained using a two-tailed statistical analysis, and $P < 0.05$ was considered statistically significant. Results are means ± S.D.

RESULTS

Down-regulation of albumin secretion and gene expression by ATRA

Among the established human HCC cell lines, FLC-4 is known to have relatively well-preserved liver cell functions, such as albumin synthesis, enzyme activity and drug metabolism [26,27]. When FLC-4 cells were incubated in the presence of ATRA for 48 h, the albumin level in the culture medium was significantly decreased in a dose-dependent manner; the inhibitory effect of ATRA at concentrations of 1, 10, 100 and 1000 nmol/l on albumin production was 37.04 ± 3.60%, 50.04 ± 3.27%, 59.96 ± 4.71% and 65.74 ± 0.74% respectively (Figure 1A). After treatment with 1000 nmol/l ATRA, the growth rate of FLC-4 cells was only slightly (approx. 30%) inhibited, and the cells exhibited no morphological changes (results not shown). To address the mechanism of down-regulation of albumin synthesis by ATRA, the mRNA level of albumin in the cells treated with ATRA for 24 h was examined. As shown in Figure 1(B), consistent with the level of the secreted protein, cellular albumin mRNA expression was inhibited significantly and dose-dependently by ATRA. A 61.95% decrease in the albumin mRNA level was observed in the presence of 100 nmol/l ATRA, demonstrating that albumin synthesis is down-regulated by ATRA via a reduction in the level of mRNA, which is presumably caused by a decrease in transcriptional activity of the albumin gene and/or albumin mRNA stability.

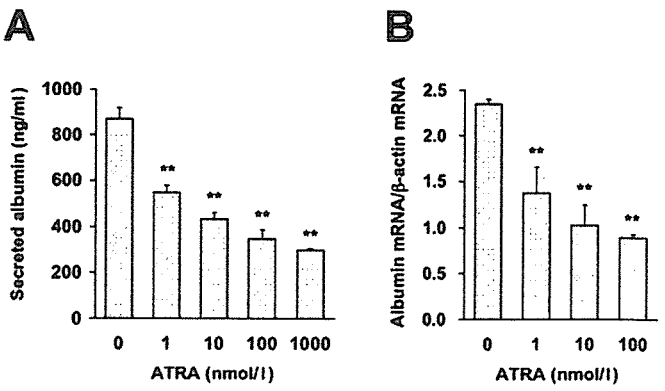

Figure 1 Effect of ATRA treatment on albumin secretion and mRNA expression in FLC-4 cells

(**A**) The culture medium was collected 48 h after the addition of ATRA. Albumin levels in the medium were quantified by ELISA. $^{**}P < 0.01$ compared with no ATRA treatment. (**B**) The cells were harvested after incubation with ATRA for 24 h. Albumin mRNA levels were measured by quantitative RT-PCR analysis. Albumin mRNA levels were normalized to β-actin mRNA levels. $^{**}P < 0.01$ compared with control cells without ATRA treatment.

Identification of the 5′ end flanking region of the albumin gene responsible for its transcriptional down-regulation by ATRA

It is well known that the effect of ATRA on the transactivation of target gene expression is mediated by retinoic acid receptors and retinoid X-receptors that bind DNA as a heterodimer [30,31]. These nuclear receptors are ligand-dependent transcription factors that bind RAREs (retinoic acid response elements) consisting of two AGGTCA sites usually arranged as DRs (direct repeats) [30,31]. The RAREs found on ATRA-regulated genes are made up of DR motifs with a spacing of 2 (DR2) or 5 nt (DR5) [31]. However, neither the consensus sequence of RAREs nor RARE-like sequences were identified in the 5′ end flanking region of the human albumin gene by sequence analysis with a computer search program, TFSEARCH (Searching Transcription Factor Binding Sites; http://www.cbrc.jp/research/db/TFSEARCH.html). One can hypothesize that the ATRA-mediated transcriptional regulation of the albumin gene is a secondary response to retinoic acid in human liver cells.

To identify the region responsible for the down-regulation of albumin gene expression by ATRA, a reporter plasmid, pAL1.9-LUC, containing a 1.9 kb fragment of the albumin 5′ end flanking sequence linked to a firefly luciferase gene was constructed (Figure 2B) and transfected into FLC-4 cells. The reporter luciferase assay demonstrated that the activity of the albumin promoter from pAL1.9-LUC was markedly decreased to 30.78% after treatment with ATRA (Figure 2B). This inhibitory effect correlated well with the inhibition of albumin mRNA expression (as shown in Figure 1B), suggesting that the 5′ end 1.9 kb flanking sequence of the albumin gene is involved in transcriptional down-regulation of albumin expression by ATRA. To define an ATRA-responsive element within the 1.9 kb fragment, a series of 5′end-deletion constructs fused with the luciferase gene were created (Figure 2B). As shown in Figure 2(B), deletions that extended to nt −367 (pAL0.4-LUC) resulted in basal promoter activities and an inhibitory effect of ATRA on promoter activity that are comparable with those observed in the cells transfected with pAL1.9-LUC. By contrast, a further deletion up to nt −167, pAL0.2-LUC, yielded a marked decrease in the basal promoter activity, as well as in the inhibitory effect of ATRA on the promoter activity. These results suggest that the region from nt −367 to −167 contains a putative element responsible for

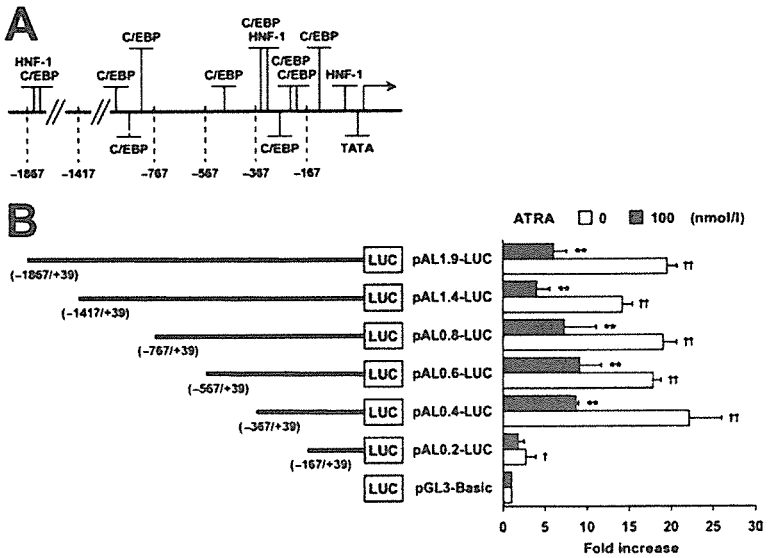

Figure 2 Identification of the 5′ end flanking region of the albumin gene responsible for its transcriptional down-regulation by ATRA

(**A**) Schematic diagram of the potential binding sites for liver-enriched transcription factors in the 5′ end flanking region of the albumin gene analysed with a computer search program, TFSEARCH. (**B**) Deletion constructs of the upstream regulatory region of the albumin gene linked to the firefly luciferase reporter gene (LUC) are shown. FLC-4 cells were co-transfected with a *Renilla* luciferase internal control reporter (pRL-CMV) and a firefly luciferase reporter. Then, cells were stimulated with (black columns) or without (white columns) 100 nmol/l ATRA for 48 h. The relative luciferase activity was obtained by normalizing the firefly luciferase activity to the *Renilla* luciferase activity. The value of the empty vector (pGL3-Basic) was set to 1. $^{**}P < 0.01$ compared with transfected cells not exposed to ATRA. $\dagger P < 0.05$; $\dagger\dagger P < 0.01$ compared with cells transfected with empty vector.

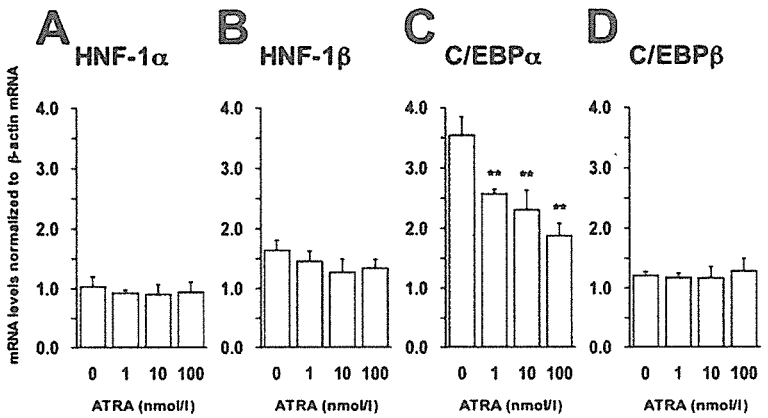

Figure 3 mRNA levels of liver-enriched transcription factors in FLC-4 cells treated with ATRA

The cells were harvested after treatment with ATRA for 24 h, and the mRNA levels of HNF-1α (**A**), HNF-1β (**B**), C/EBPα (**C**) and C/EBPβ (**D**) were measured by quantitative RT-PCR analysis. The mRNA level of each of these liver-enriched transcription factors was normalized to β-actin mRNA level. $^{**}P < 0.01$ compared with untreated control cells.

transcriptional repression by ATRA and that this region is important for a high level of expression of the human albumin gene.

Effect of ATRA on the expression of transcription factors that possibly bind to the albumin promoter

Several potential *cis*-elements within nt -367 to -167 were identified by sequence analysis using TFSEARCH. This region contained binding sites for liver-specific transcription factors, C/EBPs and HNF-1s, as indicated in Figure 2(A). We next examined whether ATRA regulates expression of these transcription factors at the transcriptional level using quantitative real-time RT-PCR (Figure 3). As shown in Figure 3(C), the mRNA level of C/EBPα, which had the most abundant expression of the four transcription factors tested, was significantly decreased by ATRA treatment in a dose-dependent manner; C/EBPα mRNA expression in FLC-4 cells was suppressed by 47 % in the presence of 100 nmol/l ATRA. By contrast, ATRA exhibited no effect or only a marginal effect on the mRNA levels of HNF-1α, HNF-1β and C/EBPβ (Figure 3A, B and D). Since C/EBPα is known to be a positive regulator of human albumin expression [32,33], it may be possible that down-regulation of C/EBPα expression is one of the mechanisms involved in the inhibitory effect of ATRA on human albumin synthesis.

In vivo recruitment of C/EBPs to the human albumin promoter

To investigate whether the inhibitory effect of ATRA on albumin expression is associated with the recruitment of C/EBPs to

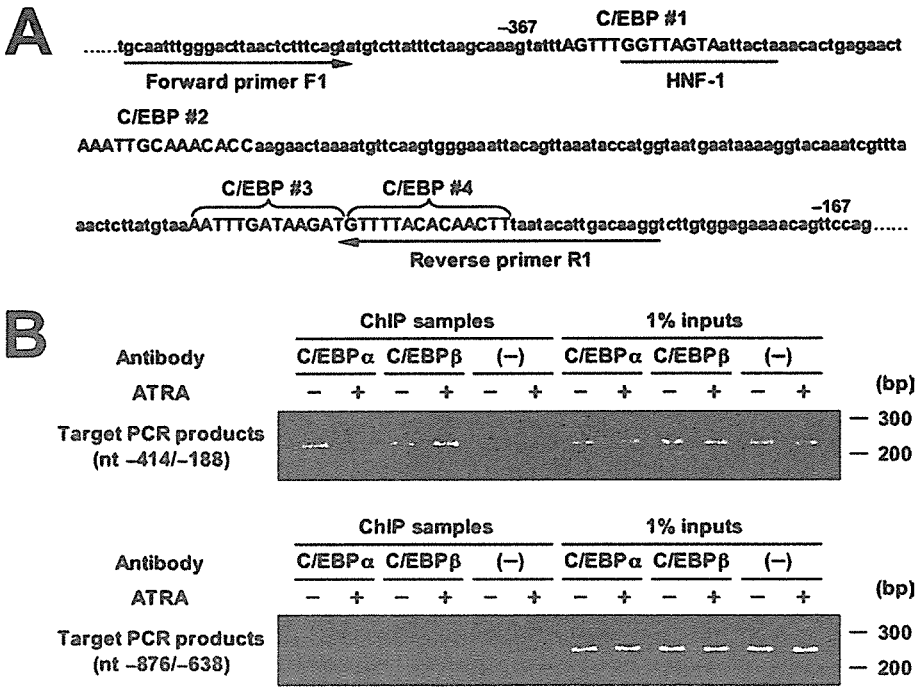

Figure 4 Effects of ATRA on *in vivo* recruitment of C/EBPs to the human albumin promoter

(**A**) The sequence of the upstream regulatory region (between nt −414 and −188) of human albumin was amplified using a PCR primer pair (F1 and R1), indicated by the arrows. The potential binding sites for C/EBP and HNF-1 in this region are in capital letters and underlined respectively. (**B**) FLC-4 cells were incubated with or without ATRA (100 nmol/l) for 48 h before the ChIP assay. DNA fragments were amplified with the primers F1 and R1 (upper panel) or F2 and R2 (lower panel). The input represents PCR products from chromatin pellets before immunoprecipitation.

the albumin promoter *in vivo*, we performed ChIP assays of cells treated with or without ATRA (Figure 4). After immunoprecipitation with antibodies against C/EBPα and C/EBPβ, the −414 to −188 nt fragment within the albumin promoter, which contains four potential binding sites for C/EBPs (C/EBP #1–#4 in Figure 4A), was amplified by PCR. The results revealed that under basal conditions both endogenous C/EBPα and C/EBPβ were recruited to the albumin promoter. It is of interest that the *in vivo* binding of C/EBPα to the fragment was markedly decreased upon incubation with ATRA. By contrast, ATRA treatment seemed to marginally increase the recruitment of C/EBPβ to the promoter fragment (Figure 4B). We verified that no DNA fragment was detected in the precipitated chromatin when the region between nt −876 and −638 of the albumin gene, which does not contain binding sites for C/EBP, was amplified by PCR.

These findings suggest that ATRA has the ability to affect the C/EBP occupancy of the albumin promoter *in vivo*. It is possible that impaired C/EBPα binding caused by ATRA leads to down-regulation of albumin gene expression.

ATRA induces expression of C/EBPβ-LIP, and its DNA-binding activity

It has been reported that the gene for C/EBP is transcribed into a single mRNA that encodes several N-terminally truncated protein isoforms, possibly via the process of alternative translation initiation at downstream AUG codons [34,35]. C/EBPα mRNA is translated into two major proteins of 42 and 30 kDa (p42- and p30-C/EBPα) [34,36], whereas C/EBPβ mRNA mainly produces three isoforms referred to as C/EBPβ-FL, LAP (liver-enriched transcriptional activator protein) and LIP, which are 46, 42, and 20 kDa respectively [34,37,38]. All of the C/EBP isoforms have DNA-binding and dimerization domains. However, p30-C/EBPα and LIP are translated from the third in-frame AUG start codon [34,36] and lack most of the transactivation domain [34,37,39]. Although p42-C/EBPα, C/EBPβ-FL and LAP transactivate their target genes' expression, p30-C/EBPα and LIP are unable to activate gene transcription and are able to function as dominant-negative factors by antagonizing and by competing with other C/EBP transactivators [34,37]. It has been considered that the ratio of C/EBP transactivators to C/EBP dominant-negative factors is important in controlling each activity of C/EBPα and C/EBPβ [34,36,37].

We determined the effect of ATRA on the expression of C/EBP isoforms by Western blotting (Figure 5A). An increased level of LIP was observed as early as 8 h after ATRA treatment and it was also detected after 48 h of treatment. By contrast, C/EBPβ-FL and LAP isoforms showed little change in their expression after the 48 h time point of ATRA treatment. The expression level of C/EBPα showed no change in the presence of ATRA after 8 or 16 h. Although a decrease in C/EBPα expression was found after 48 h of ATRA treatment, it is not likely that this reduction is the cause of down-regulation of albumin expression, since a decreased level of albumin mRNA was observed as early as 24 h after ATRA treatment (Figure 1B). It appears that the ratio of LIP to C/EBPβ-FL and LAP was elevated in a dose-dependent manner after 16 h of ATRA treatment, while the ratio of p42-C/EBPα to p30-C/EBPα showed no difference with or without ATRA treatment until 48 h after the addition of ATRA. These results demonstrate that ATRA has the ability to differentially modulate the level of C/EBP isoforms with an increase in LIP and a decrease in C/EBPα; the expression of LIP is induced immediately in response to ATRA treatment.

We next examined the effect of ATRA on the DNA-binding activity of LIP, by EMSA (Figure 5B). The nucleotide sequence of C/EBP-binding site #3, which is present in the region from

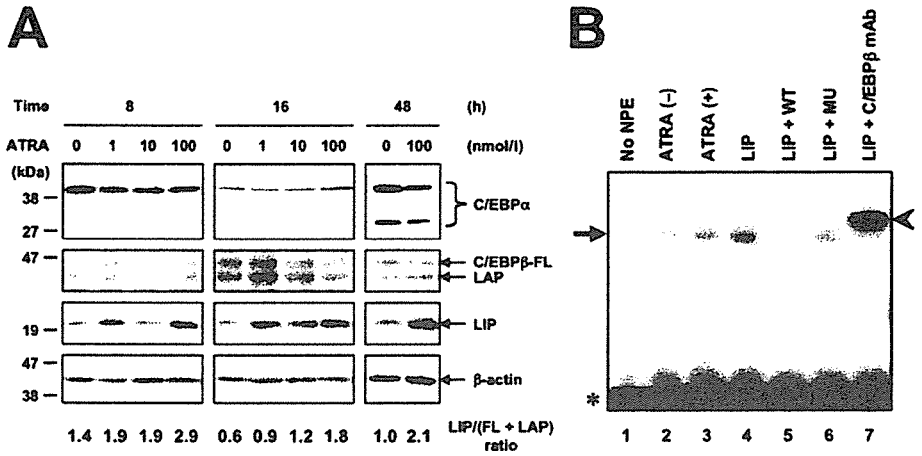

Figure 5 Effect of ATRA on protein expression of C/EBPs, and DNA-binding activity of C/EBPβ-LIP

(**A**) FLC-4 cells were incubated with ATRA (100 nmol/l) for 8, 16 and 48 h. After harvesting, total cellular proteins were resolved by SDS/PAGE, and the presence of C/EBPα and C/EBPβ was analysed by Western blotting. The ratio of C/EBPβ-LIP to C/EBPβ-FL and -LAP [LIP/(FL + LAP)] was measured by densitometric analysis. (**B**) Nuclear proteins were extracted from FLC-4 cells treated with or without 100 nmol/l ATRA for 48 h, or cells that transiently expressed the LIP protein, and were analysed by EMSA as described in the Experimental section. Lane 1, no nuclear protein extracts (NPE); lane 2, FLC-4 cells incubated without ATRA; lane 3, FLC-4 cells incubated with ATRA; lane 4, FLC-4 cells transiently expressing the LIP protein; lane 5, addition of a 50-fold molar excess of unlabelled wild-type (WT) oligonucleotides to the mixture in lane 4; lane 6, addition of a 50-fold molar excess of unlabelled mutant (MU) oligonucleotides to the mixture in lane 4; lane 7, addition of an anti-C/EBPβ monoclonal antibody (mAb) to the mixture in lane 4. The arrow, arrowhead and asterisk indicate a DNA–LIP complex, a DNA–LIP-antibody complex (supershifted band) and a free probe respectively.

nt -367 to -167 of the albumin gene, as shown in Figure 4(A), was used as a DNA probe. A shifted band, which was observed in FLC-4 cells that transiently express LIP protein (Figure 5, lane 4), was removed by the addition of an excess of unlabelled homologous probe (lane 5), but not by the addition of a mutated sequence (lane 6). This band was supershifted by the addition of the C/EBPβ antibody (lane 7). The results indicate that LIP binds to its binding motif within the albumin promoter.

In the presence of ATRA (Figure 5, lane 3), a shifted band that corresponded to endogenous LIP-bound DNA was observed, which was more intense than in the absence of ATRA (lane 2). We also confirmed that endogenous LIP bound to the other three binding sites for C/EBP (#1, #2 and #4) (results not shown). Thus the combined data demonstrate that ATRA induces not only the expression of LIP but also its DNA-binding activity.

C/EBPβ-LIP down-regulates the gene expression and synthesis of albumin by blocking the transcriptional activity of C/EBPα and C/EBPβ-FL

Our data suggest that early induction of LIP expression and an increase in the DNA-binding activity of LIP caused by ATRA triggers the down-regulation of albumin gene expression. To directly evaluate the role of LIP in albumin expression, we determined the effect of C/EBPs on albumin expression using transient transfection experiments (Figure 6). As shown in Figure 6(A), overexpression of C/EBPα and C/EBPβ-FL caused a more than 20.7- or 8-fold increase respectively, in promoter activity in a dose-dependent manner compared with transfection with an empty vector. By contrast, co-expression with LIP resulted in a marked and dose-dependent reduction of the increased activity (Figure 6B). Expression of LIP alone also decreased the level of promoter activity (Figure 6B), presumably because LIP inhibited positive functions of endogenous C/EBP transactivators expressed in FLC-4 cells. We investigated the effect of C/EBP expression on the secretion of endogenous albumin (Figure 6C). Consistent with albumin promoter activity, overexpression of C/EBPα and C/EBPβ-FL significantly increased the level of albumin in the culture mediun by 2- and 1.7-fold respectively, compared with transfection with an empty vector. Overexpression of LIP significantly and dose-dependently decreased both the basal level of albumin secretion and the level of albumin elevated by expression of C/EBPα and C/EBPβ-FL. Thus these results strongly suggest that LIP plays a role in repressing albumin gene expression by blocking the ability of C/EBP transactivators to activate the albumin promoter, leading to down-regulation of albumin synthesis.

DISCUSSION

In the present study, we have demonstrated the down-regulation of secretion and gene expression of albumin mediated by ATRA. This finding is in line with previous reports that ATRA negatively regulates albumin synthesis in rat hepatocytes [20] and human hepatoma cell lines [12,13]. We addressed its molecular mechanisms and found: (i) that the 5′ end flanking region of the albumin gene, nt -367 to -167, in which four binding sites for C/EBPs are conserved, is responsible for its transcriptional repression by ATRA, and (ii) that upon ATRA treatment, C/EBPβ-LIP is differentially induced among C/EBPβ isoforms and the expression of C/EBPα is subsequently decreased. The present study reveals that C/EBP proteins play a key role in the transcriptional regulation of the human albumin gene by ATRA.

C/EBPα and C/EBPβ, which are composed of DNA-binding and dimerization domains at their C-termini, and transactivation domains at their N-terminal regions, are expressed in the liver at high levels and are involved in the regulation of cell growth, cell differentiation, metabolism and inflammation [40–42]. A single mRNA species for C/EBPβ directs production of three major isoforms in liver tissues: C/EBPβ-FL, LAP and a low-molecular-mass isoform, LIP [34,37,38]. These three proteins contain the DNA-binding and dimerization domains. C/EBPβ-FL and LAP contain a transactivation domain and function as transcriptional activators, whereas LIP lacks the N-terminal transactivation domain and can attenuate the transcriptional stimulation by

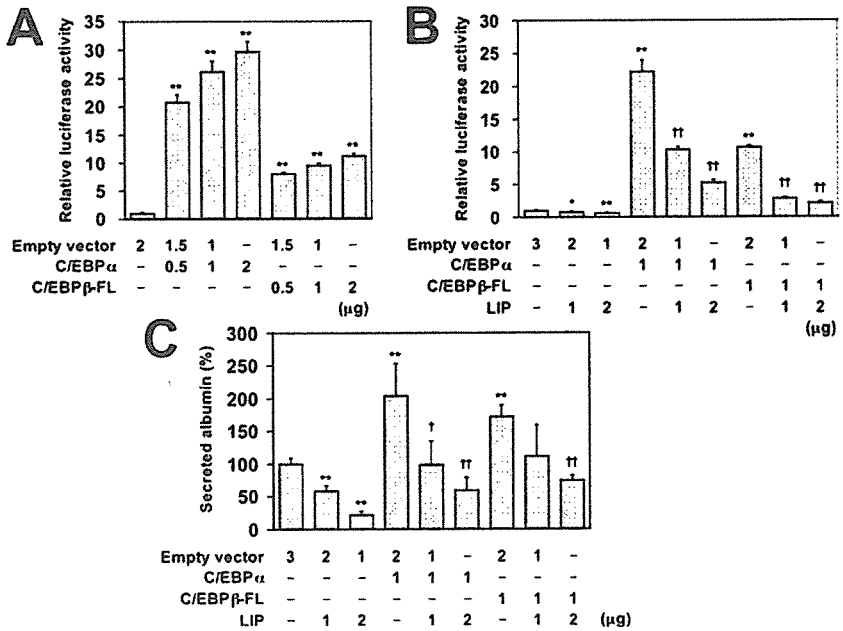

Figure 6 C/EBPβ-LIP down-regulates the promoter activity and synthesis of albumin by blocking C/EBP transcriptional activity

(**A**) and (**B**) FLC-4 cells were transfected with pAL1.9-LUC and pRL-CMV in the presence or absence of C/EBP expression vectors. After incubation for 48 h, the cells were harvested and assayed for luciferase activity. The relative luciferase activity was obtained by normalizing the pAL1.9-LUC activity to the pRL-CMV activity, and the value of the empty vector (pCAGGS) was set to 1. $*P < 0.05$; $**P < 0.01$ compared with cells transfected with empty vector. $\dagger\dagger P < 0.01$ compared with cells expressing C/EBPα or C/EBPβ-FL alone. (**C**) FLC-4 cells were transfected with C/EBP expression vectors and/or an empty vector. After 72 h, the medium was harvested, and the amount of secreted albumin was quantified by ELISA. The value of the empty vector was set to 100 %. $**P < 0.01$ compared with transfection with empty vector. $\dagger P < 0.05$; $\dagger\dagger P < 0.01$ compared with cultures that express C/EBPα or C/EBPβ-FL alone.

C/EBPβ-FL, LAP and C/EBPα in substoichiometric amounts [37]. It has been shown that LIP is involved in the down-regulation of human *CYP3A4* induced by interleukin-6 [43] and in the repression of C/EBPα mRNA during the acute phase of the immune response [44]. In the present study, we have demonstrated that the overexpression of LIP leads to inhibition of the positive regulation of albumin promoter activity that is mediated by C/EBPα and C/EBPβ-FL (Figure 6B). This is the first study to show the involvement of LIP in the regulation of human albumin gene expression.

Our albumin promoter assay using the 5′end-deletion constructs demonstrated that the region spanning nt −367 to −167 within the albumin gene is a prerequisite for ATRA-dependent transcriptional down-regulation (Figure 2B). The ChIP assay showed that during ATRA treatment the *in vivo* binding of C/EBPα to the region clearly decreased, whereas the binding of C/EBPβ slightly increased (Figure 4B). The anti-C/EBPβ antibody used in the present study is capable of recognizing all of the C/EBPβ isoforms, since no anti-C/EBPβ antibodies that recognize the N-termini of C/EBPβ are available to distinguish these isoforms. However, an EMSA demonstrated that ATRA increased the binding activity of LIP to its response element in this region (Figure 5B). Thus we suggest that the increase in DNA-binding of C/EBPβ, as shown in the ChIP assay, is caused by ATRA-induced LIP expression. It has been reported that LIP has a greater binding capacity for the C/EBP-binding element compared with C/EBP transactivators i.e. LIP binds to the element 4-fold more efficiently than does LAP [37]. Therefore it is probable that C/EBP transactivators predominantly bind to their response elements within the albumin promoter in the ATRA-untreated cells, while an increased level of LIP possibly displaces these transactivators at the C/EBP-binding sites to occuy them in ATRA-treated cells.

As indicated in Figure 5(A), preferential induction of LIP expression by ATRA was observed even in the culture after

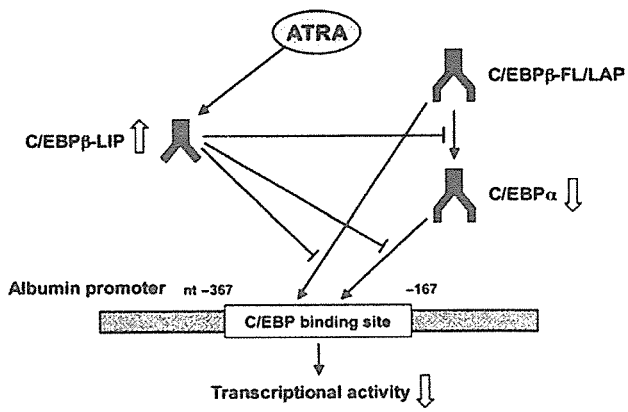

Figure 7 Proposed mechanism by which ATRA down-regulates albumin gene transcription in FLC-4 cells

An ATRA signal increases the expression of C/EBPβ-LIP in FLC-4 cells. This truncated C/EBP protein directly and indirectly down-regulates the expression of the albumin gene by competing with C/EBP transactivators and inhibiting C/EBPα expression.

8 h of ATRA treatment. By contrast, a decrease in C/EBPα gene expression was not detected at such an early stage (results not shown), but was first observed 24 h after the addition of ATRA (Figure 3C). Furthermore, the expression level of C/EBPα protein was little changed when the mRNA expression level of albumin was decreased by ATRA treatment (Figure 5A). Based on the results of the present study, we propose a model for the molecular mechanism by which ATRA down-regulates the expression of human albumin in liver-derived cells (Figure 7). ATRA triggers the differential induction of C/EBPβ-LIP, a dominant-negative regulator of C/EBP activators. A C/EBP-binding consensus sequence has been identified in the C/EBPα

promoter, and it has been shown that C/EBPβ-FL and LIP respectively, function as positive and negative regulators of C/EBPα gene expression [44]. Thus it is probable that LIP preferentially binds to the C/EBP-binding elements not only on the albumin promoter but also on that of C/EBPα at the expense of C/EBPβ-FL, LAP and C/EBPα. However, LIP lacks the transactivation domain and is unable to activate transcription. LIP expression induced by ATRA possibly down-regulates the gene expression of albumin and C/EBPα, by competing for DNA-binding sites as a LIP homodimer and/or by antagonizing the transcriptional activity of C/EBP transactivators via heterodimer formation with C/EBP-FL or LAP [37]. Hence, an increase in the ratio of LIP to C/EBP transactivators is critical for down-regulation of the expression of albumin and C/EBPα genes that is mediated by ATRA. This conclusion is supported by transient transfection experiments which indicated that the activity of the albumin promoter is stimulated by transfection with C/EBPβ-FL or C/EBPα expression constructs (Figure 6A), whereas its activity is decreased by co-transfection with a LIP construct (Figure 6B). Decreased expression of C/EBPα may also contribute to the transcriptional repression of the albumin gene, since C/EBPα is known to be one of the positive regulators of albumin expression [32,33].

A key question is: how does ATRA differentially induce C/EBPβ-LIP but not C/EBPβ-FL expression? A previous study [45], which describes the effect of ATRA on the alternate production of C/EBPβ isoforms, has not demonstrated its molecular mechanism. A number of recent observations have shown that the production of C/EBPβ isoforms is regulated by epidermal growth factor [38], lipopolysacharide [44,46] and partial hepatectomy [44,47], presumably through leaky ribosomal scanning [34,37]. It has been proposed that a portion of ribosomes ignore the first two AUG codons of the C/EBPβ mRNA and initiate translation of LIP from the third in-frame AUG start codon. The translation of LIP can be controlled by specific cytoplasmic proteins that interact with the 5′ end region of C/EBPβ mRNA, such as CUG-BP1 (CUG triplet-repeat binding protein 1) [44,47]. Phosphorylation of CUG-BP1 is critical for its RNA binding and the consequent increase in LIP expression [38]. Therefore we tested whether ATRA treatment leads to increased phosphorylation of CUG-BP1 in FLC-4 cells. Western blotting and immunoprecipitation of CUG-BP1 metabolically labelled with ^{32}P, however, indicated that the expression level and phosphorylation status of CUG-BP1 were not different in cells with or without ATRA treatment (results not shown). It can be speculated that other RNA-binding proteins are involved in the mechanism by which ATRA increases the translation of LIP because, in addition to CUG-BP1, calreticulin [48] and eIFs (eukaryotic translation initiation factors), such as eIF-2 and eIF-4E [35], have been shown to control translation of C/EBPβ. Another possible mechanism for the alternate production of C/EBPβ isoforms is the proteolytic cleavage of C/EBPβ-FL [49]. However, this is less likely to explain the mechanism for the differential induction of LIP isoforms caused by ATRA, because it has been shown that the cleavage of C/EBPβ-FL to generate LIP is induced by C/EBPα [49], but that the ATRA treatment led to no change or only a small decrease in the expression of C/EBPα (Figure 5A).

A previous study [13] has shown that the expression of HNF-1, which is a potent transcription factor for the albumin gene [50], was decreased in human hepatoma cells in which albumin gene expression was down-regulated by ATRA, although an upstream regulatory region of the albumin gene involved in the regulation was not identified. In our experimental setting, mRNA expression of HNF-1 was not affected by ATRA treatment (Figures 3A and 3B). The data in the present study suggest a model in which the preferential increase in LIP expression mediated by ATRA results in the antagonization of C/EBP transactivators by interaction with their binding sites on the nt −367 to −167 region of the albumin promoter. We propose a novel pathway for the modulation of gene expression by ATRA, in which C/EBPβ-LIP plays a crucial role. This mechanism may be found in other systems for physiological processes, such as cell proliferation and differentiation, and the elucidation of its molecular mechanism will make a great contribution to our understanding of gene regulation mediated by retinoic acids.

We thank G. J. Darlington for providing the plasmids, and A. Catharine Ross (Department of Nutritional Sciences, The Pennsylvania State University) and our colleagues for helpful discussions. We also thank M. Matsuda, M. Ikeda, S. Yoshizaki and T. Shimoji for their technical assistance. This work was supported by grants-in-aid from the Ministry of Health, Labor and Welfare, by the Program for Promotion of Fundamental Studies in Health Sciences of the Organization for Drug ADR Relief, R&D Promotion and Product Review of Japan (ID:01-3), and by Research on Health Sciences focusing on Drug Innovation from the Japan Health Sciences Foundation, Japan. T. M. is the recipient of a Research Resident Fellowship from the Foundation for Promotion of Cancer Research in Japan.

REFERENCES

1 West, J. B. (1990) Blood and the plasma proteins: functions and composition of blood. In Physiological Basis of Medical Practice. In (West, J. B., ed.), pp. 332–338, Williams & Wilkins, Baltimore
2 Rothschild, M. A., Oratz, M. and Schreiber, S. S. (1988) Serum albumin. Hepatology **8**, 385–401
3 Moshage, H. J., Janssen, J. A., Franssen, J. H., Hafkenscheid, J. C. and Yap, S. H. (1987) Study of the molecular mechanism of decreased liver synthesis of albumin in inflammation. J. Clin. Invest. **79**, 1635–1641
4 Mariani, G., Strober, W., Keiser, H. and Waldmann, T. A. (1976) Pathophysiology of hypoalbuminemia associated with carcinoid tumor. Cancer **38**, 854–860
5 Chlebowski, R. T., Grosvenor, M. B., Bernhard, N. H., Morales, L. S. and Bulcavage, L. M. (1989) Nutritional status, gastrointestinal dysfunction, and survival in patients with AIDS. Am. J. Gastroenterol. **84**, 1288–1293
6 Phillips, A., Shaper, A. G. and Whincup, P. H. (1989) Association between serum albumin and mortality from cardiovascular disease, cancer, and other causes. Lancet **2**, 1434–1436
7 Gorski, K., Carneiro, M. and Schibler, U. (1986) Tissue-specific *in vitro* transcription from the mouse albumin promoter. Cell **47**, 767–776
8 Maire, P., Wuarin, J. and Schibler, U. (1989) The role of *cis*-acting promoter elements in tissue-specific albumin gene expression. Science **244**, 343–346
9 Perlmutter, D. H., Dinarello, C. A., Punsal, P. I. and Colten, H. R. (1986) Cachectin/tumor necrosis factor regulates hepatic acute-phase gene expression. J. Clin. Invest. **78**, 1349–1354
10 Andus, T., Geiger, T., Hirano, T., Kishimoto, T. and Heinrich, P. C. (1988) Action of recombinant human interleukin 6, interleukin 1β and tumor necrosis factor α on the mRNA induction of acute-phase proteins. Eur. J. Immunol. **18**, 739–746
11 Morrone, G., Cortese, R. and Sorrentino, V. (1989) Post-transcriptional control of negative acute phase genes by transforming growth factor β. EMBO J. **8**, 3767–3771
12 Hsu, S. L., Lin, Y. F. and Chou, C. K. (1992) Transcriptional regulation of transferrin and albumin genes by retinoic acid in human hepatoma cell line Hep3B. Biochem. J. **283**, 611–615
13 Yamada, Y., Shidoji, Y., Fukutomi, Y., Ishikawa, T., Kaneko, T., Nakagama, H., Imawari, M., Moriwaki, H. and Muto, Y. (1994) Positive and negative regulations of albumin gene expression by retinoids in human hepatoma cell lines. Mol. Carcinog. **10**, 151–158
14 Molina, A., Oka, T., Muñoz, S. M., Chikamori-Aoyama, M., Kuwahata, M. and Natori, Y. (1997) Vitamin B_6 suppresses growth and expression of albumin gene in a human hepatoma cell line HepG2. Nutr. Cancer **28**, 206–211
15 Tsutsumi, T., Nakao, K., Mitsuoka, S., Hamasaki, K., Tsuruta, S., Shima, M., Nakata, K., Tamaoki, T. and Nagataki, S. (1993) Regulation of albumin and α-fetoprotein gene expression by colloid osmotic pressure in human hepatoma cells. Gastroenterology **104**, 256–262
16 Pietrangelo, A. and Shafritz, D. A. (1994) Homeostatic regulation of hepatocyte nuclear transcription factor 1 expression in cultured hepatoma cells. Proc. Natl. Acad. Sci. U.S.A. **91**, 182–186
17 Marten, N. W., Hsiang, C. H., Yu, L., Stollenwerk, N. S. and Straus, D. S. (1999) Functional activity of hepatocyte nuclear factor-1 is specifically decreased in amino acid-limited hepatoma cells. Biochim. Biophys. Acta **1447**, 160–174

18 Falasca, L., Favale, A., Gualandi, G., Maietta, G. and Conti Devirgiliis, L. (1998) Retinoic acid treatment induces apoptosis or expression of a more differentiated phenotype on different fractions of cultured fetal rat hepatocytes. Hepatology **28**, 727–737
19 Alisi, A., Leoni, S., Piacentani, A. and Conti Devirgiliis, L. (2003) Retinoic acid modulates the cell-cycle in fetal rat hepatocytes and HepG2 cells by regulating cyclin-cdk activities. Liver Int. **23**, 179–186
20 Ikeda, H. and Fujiwara, K. (1993) Retinoic acid inhibits DNA and albumin synthesis stimulated by growth factor in adult rat hepatocytes in primary culture. Biochem. Biophys. Res. Commun. **191**, 675–680
21 Sani, B. P. and Meeks, R. G. (1983) Subacute toxicity of all-*trans*- and 13-*cis*-isomers of *N*-ethyl retinamide, *N*-2-hydroxyethyl retinamide, and *N*-4-hydroxyphenyl retinamide. Toxicol. Appl. Pharmacol. **70**, 228–235
22 Decensi, A., Bruno, S., Costantini, M., Torrisi, R., Curotto, A., Gatteschi, B., Nicolò, G., Polizzi, A., Perloff, M., Malone, W. F. and Bruzzi, P. (1994) Phase IIa study of fenretinide in superficial bladder cancer, using DNA flow cytometry as an intermediate end point. J. Natl. Cancer Inst. **86**, 138–140
23 Kalemkerian, G. P., Slusher, R., Ramalingam, S., Gadgeel, S. and Mabry, M. (1995) Growth inhibition and induction of apoptosis by fenretinide in small-cell lung cancer cell lines. J. Natl. Cancer Inst. **87**, 1674–1680
24 Maurer, B. J., Metelitsa, L. S., Seeger, R. C., Cabot, M. C. and Reynolds, C. P. (1999) Increase of ceramide and induction of mixed apoptosis/necrosis by *N*-(4-hydroxyphenyl)-retinamide in neuroblastoma cell lines. J. Natl. Cancer Inst. **91**, 1138–1146
25 Puduvalli, V. K., Yung, W. K., Hess, K. R., Kuhn, J. G., Groves, M. D., Levin, V. A., Zwiebel, J., Chang, S. M., Cloughesy, T. F., Junck, L. et al. (2004) Phase II study of fenretinide (NSC 374551) in adults with recurrent malignant gliomas: a North American brain tumor consortium study. J. Clin. Oncol. **22**, 4282–4289
26 Nagamori, S., Hasumura, S., Matsuura, T., Aizaki, H. and Kawada, M. (2000) Developments in bioartificial liver research: concepts, performance, and applications. J. Gastroenterol. **35**, 493–503
27 Aizaki, H., Nagamori, S., Matsuda, M., Kawakami, H., Hashimoto, O., Ishiko, H., Kawada, M., Matsuura, T., Hasumura, S., Matsuura, Y. et al. (2003) Production and release of infectious hepatitis C virus from human liver cell cultures in the three-dimensional radial-flow bioreactor. Virology **314**, 16–25
28 Niwa, H., Yamamura, K. and Miyazaki, J. (1991) Efficient selection for high-expression transfectants with a novel eukaryotic vector. Gene **108**, 193–199
29 Iwahori, T., Matsuura, T., Maehashi, H., Sugo, K., Saito, M., Hosokawa, M., Chiba, K., Masaki, T., Aizaki, H., Ohkawa, K. and Suzuki, T. (2003) CYP3A4 inducible model for *in vitro* analysis of human drug metabolism using a bioartificial liver. Hepatology **37**, 665–673
30 Mangelsdorf, D. J. and Evans, R. M. (1995) The RXR heterodimers and orphan receptors. Cell **83**, 841–850
31 Chambon, P. (1996) A decade of molecular biology of retinoic acid receptors. FASEB J. **10**, 940–954
32 Friedman, A. D., Landschulz, W. H. and McKnight, S. L. (1989) CCAAT/enhancer binding protein activates the promoter of the serum albumin gene in cultured hepatoma cells. Genes Dev. **3**, 1314–1322
33 Trautwein, C., Rakemann, T., Pietrangelo, A., Plümpe, J., Montosi, G. and Manns, M. P. (1996) C/EBP-β/LAP controls down-regulation of albumin gene transcription during liver regeneration. J. Biol. Chem. **271**, 22262–22270
34 Ossipow, V., Descombes, P. and Schibler, U. (1993) CCAAT/enhancer-binding protein mRNA is translated into multiple proteins with different transcription activation potentials. Proc. Natl. Acad. Sci. U.S.A. **90**, 8219–8223
35 Calkhoven, C. F., Müller, C. and Leutz, A. (2000) Translational control of C/EBPα and C/EBPβ isoform expression. Genes Dev. **14**, 1920–1932
36 Lin, F. T., MacDougald, O. A., Diehl, A. M. and Lane, M. D. (1993) A 30-kDa alternative translation product of the CCAAT/enhancer binding protein α message: transcriptional activator lacking antimitotic activity. Proc. Natl. Acad. Sci. U.S.A. **90**, 9606–9610
37 Descombes, P. and Schibler, U. (1991) A liver-enriched transcriptional activator protein, LAP, and a transcriptional inhibitory protein, LIP, are translated from the same mRNA. Cell **67**, 569–579
38 Baldwin, B. R., Timchenko, N. A. and Zahnow, C. A. (2004) Epidermal growth factor receptor stimulation activates the RNA binding protein CUG-BP1 and increases expression of C/EBPβ-LIP in mammary epithelial cells. Mol. Cell. Biol. **24**, 3682–3691
39 Calkhoven, C. F., Bouwman, P. R., Snippe, L. and Ab, G. (1994) Translation start site multiplicity of the CCAAT/enhancer binding protein α mRNA is dictated by a small 5′ open reading frame. Nucleic Acids Res. **22**, 5540–5547
40 Wang, N. D., Finegold, M. J., Bradley, A., Ou, C. N., Abdelsayed, S. V., Wilde, M. D., Taylor, L. R., Wilson, D. R. and Darlington, G. J. (1995) Impaired energy homeostasis in C/EBPα knockout mice. Science **269**, 1108–1112
41 Poli, V. (1998) The role of C/EBP isoforms in the control of inflammatory and native immunity functions. J. Biol. Chem. **273**, 29279–29282
42 Wang, H., Iakova, P., Wilde, M., Welm, A., Goode, T., Roesler, W. J. and Timchenko, N. A. (2001) C/EBPα arrests cell proliferation through direct inhibition of Cdk2 and Cdk4. Mol. Cell **8**, 817–828
43 Jover, R., Bort, R., Gómez-Lechón, M. J. and Castell, J. V. (2002) Down-regulation of human CYP3A4 by the inflammatory signal interleukin 6: molecular mechanism and transcription factors involved. FASEB J. **16**, 1799–1801
44 Welm, A. L., Mackey, S. L., Timchenko, L. T., Darlington, G. J. and Timchenko, N. A. (2000) Translational induction of liver-enriched transcriptional inhibitory protein during acute phase response leads to repression of CCAAT/enhancer binding protein α mRNA. J. Biol. Chem. **275**, 27406–27413
45 Hsu, W. and Chen-Kiang, S. (1993) Convergent regulation of NF-IL6 and Oct-1 synthesis by interleukin-6 and retinoic acid signaling in embryonal carcinoma cells. Mol. Cell. Biol. **13**, 2515–2523
46 Hsieh, C. C., Xiong, W., Xie, Q., Rabek, J. P., Scott, S. G., An, M. R., Reisner, P. D., Kuninger, D. T. and Papaconstantinou, J. (1998) Effects of age on the posttranscriptional regulation of CCAAT/enhancer binding protein α and CCAAT/enhancer binding protein β isoform synthesis in control and LPS-treated livers. Mol. Biol. Cell **9**, 1479–1494
47 Timchenko, N. A., Welm, A. L., Lu, X. and Timchenko, L. T. (1999) CUG repeat binding protein (CUGBP1) interacts with the 5′ region of C/EBPβ mRNA and regulates translation of C/EBPβ isoforms. Nucleic Acids Res. **27**, 4517–4525
48 Timchenko, L. T., Iakova, P., Welm, A. L., Cai, Z. J. and Timchenko, N. A. (2002) Calreticulin interacts with C/EBPα and C/EBPβ mRNAs and represses translation of C/EBP proteins. Mol. Cell. Biol. **22**, 7242–7257
49 Welm, A. L., Timchenko, N. A. and Darlington, G. J. (1999) C/EBPα regulates generation of C/EBPβ isoforms through activation of specific proteolytic cleavage. Mol. Cell. Biol. **19**, 1695–1704
50 Lichtsteiner, S. and Schibler, U. (1989) A glycosylated liver-specific transcription factor stimulates transcription of the albumin gene. Cell **57**, 1179–1187

Received 21 November 2005/20 March 2006; accepted 11 April 2006
Published as BJ Immediate Publication 11 April 2006, doi:10.1042/BJ20051863

J. Biochem. 139, 921–930 (2006)
doi:10.1093/jb/mvj104

Proteomic Profiling of Lipid Droplet Proteins in Hepatoma Cell Lines Expressing Hepatitis C Virus Core Protein

Shigeko Sato[1], Masayoshi Fukasawa[1,*], Yoshio Yamakawa[1], Tohru Natsume[2], Tetsuro Suzuki[3], Ikuo Shoji[3], Hideki Aizaki[3], Tatsuo Miyamura[3] and Masahiro Nishijima[1,†]

[1]Department of Biochemistry and Cell Biology and [3]Department of Virology II, National Institute of Infectious Diseases, Tokyo 162-8640; and [2]National Institute of Advanced Industrial Science and Technology (AIST), Biological Information Research Center, Tokyo 135-0064

Received February 7, 2006; accepted April 4, 2006

Hepatitis C virus (HCV) core protein has been suggested to play crucial roles in the pathogeneses of liver steatosis and hepatocellular carcinomas due to HCV infection. Intracellular HCV core protein is localized mainly in lipid droplets, in which the core protein should exert its significant biological/pathological functions. In this study, we performed comparative proteomic analysis of lipid droplet proteins in core-expressing and non-expressing hepatoma cell lines. We identified 38 proteins in the lipid droplet fraction of core-expressing (Hep39) cells and 30 proteins in that of non-expressing (Hepswx) cells by 1-D-SDS-PAGE/MALDI-TOF mass spectrometry (MS) or direct nanoflow liquid chromatography–MS/MS. Interestingly, the lipid droplet fraction of Hep39 cells had an apparently lower content of adipose differentiation–related protein and a much higher content of TIP47 than that of Hepswx cells, suggesting the participation of the core protein in lipid droplet biogenesis in HCV-infected cells. Another distinct feature is that proteins involved in RNA metabolism, particularly DEAD box protein 1 and DEAD box protein 3, were detected in the lipid droplet fraction of Hep39 cells. These results suggest that lipid droplets containing HCV core protein may participate in the RNA metabolism of the host and/or HCV, affecting the pathopoiesis and/or virus replication/production in HCV-infected cells.

Key words: ADRP, DEAD box protein, hepatitis C virus, lipid droplet, TIP47.

Abbreviations: HCV, hepatitis C virus; HCC, hepatocellular carcinoma; MS, mass spectrometry; DNLC, direct nanoflow liquid chromatography; HRP, horseradish peroxidase; ADRP, adipose differentiation–related protein; DDX1, DEAD box protein 1; DDX3, DEAD box protein 3.

Hepatitis C virus (HCV) is a major causative agent of chronic hepatitis (*1*, *2*). Persistent HCV infection, which occurs in more than 70% of infected patients, is strongly associated with the development of liver steatosis, which involves the accumulation of intracellular lipid droplets, cirrhosis, and hepatocellular carcinomas (HCC) (*3*, *4*). Since more than 170 million people in the world are currently infected with HCV (*1*), and there is no cure that is completely effective, understanding the mechanism by which HCV induces serious liver diseases is one of the most important global public health issues. HCV, a member of the *Flaviviridae* family, possesses a single-stranded, positive-sense RNA genome of ~9.6 kb (*5*). The HCV genome has a single open reading frame that codes for a large precursor polyprotein of ~3,000 amino acids that is processed into at least 10 individual proteins by host and viral proteases (*6*).

HCV core protein, the product of the N-terminal portion of the polyprotein, generated upon cleavage at the endoplasmic reticulum by signal peptidase and signal peptide peptidase (*7*, *8*), forms the nucleocapsid of an HCV virion (*9*). Interestingly, in addition to its function as a structural protein, the core protein exhibits activities leading host cells to lipogenic and malignant transformation *in vitro* (*10–12*). Moreover, transgenic mice expressing HCV core protein developed liver steatosis and HCC (*13*, *14*), suggesting an important role of the core protein in these diseases. Many studies have shown that HCV core protein substantially affects various cellular regulatory processes, such as gene transcription (*15–17*) and signal transduction pathways (*12*, *18–23*), and interacts with a variety of host proteins (*12*, *18*, *19*, *22*, *24–34*), but it is not clear what activities/molecules are practically relevant to the pathogeneses of HCV (core)-derived liver steatosis and HCC. Extensive screenings for genes/proteins exhibiting differences in cellular expression by cDNA microarray (*35–40*) or proteome analysis (*41*, *42*) have also been tried for HCV-related HCC. Although various genes/proteins were identified, further studies are required to identify the molecules eventually involved in the pathogenesis of HCV-related HCC.

In host cells, HCV core protein is distributed mainly in lipid droplets and the endoplasmic reticulum (*7*, *10*, *43–46*), in which the core protein is predicted to exert its significant biological/pathological functions. In this study, we thus focused on HCV core protein and lipid droplets, and

*To whom correspondence should be addressed. Tel: +81-3-5285-1111, Fax: +81-3-5285-1157, E-mail: fuka@nih.go.jp
†Present address: Department of Clinical Pharmacy, Faculty of Pharmaceutical Sciences, Doshisha Women's College of Liberal Arts, Kyoto 610-0395.

performed comparative targeted proteomic analysis of the lipid droplet proteins in HCV core–expressing and non-expressing hepatoma cell lines using two strategies: conventional 1-D-SDS-PAGE/MALDI-TOF mass spectrometry (MS) and automated high-throughput direct nanoflow liquid chromatography (DNLC)–MS/MS. We found prominent differences in the protein compositions of lipid droplets between HCV core–expressing and non-expressing hepatoma cell lines.

MATERIALS AND METHODS

Cell Lines—The human hepatoma HepG2 cell line constitutively expressing HCV core protein (Hep39) was established as described previously (*47*). Another HepG2 cell line transfected with expression vector pcEF321swxneo without the HCV core protein insert (Hepswx) was used as a mock control (*47*). Both cell lines were plated on collagen-coated dishes (Asahi Techno Glass, Tokyo, Japan) and maintained in the normal culture medium [DMEM supplemented with 10% fetal bovine serum, 100 units/ml Penicillin G, 100 μg/ml streptomycin sulfate, and 1 mg/ml G418 (Sigma, St. Louis, MO, USA)] under a 5% CO_2 atmosphere at 37°C.

Lipid Droplet Preparation—Hepswx and Hep39 cells were seeded at 4×10^6 cells/dish (150 mm, inner diameter) in 25 ml of normal culture medium and cultured for one day. For efficient formation of lipid droplets by cells, cholesterol (final 20 μg/ml) and oleic acid (final 400 μM)/fatty acid–free BSA (final 60 μM) complex, prepared as stock solutions of 5 mg/ml cholesterol in ethanol and 10 mM oleic acid/1.5 mM BSA in PBS, respectively, were added to the medium. Each cell line was further incubated for 48–72 h at 37°C. For proteomic analysis of lipid droplet proteins, confluent monolayers of Hepswx and Hep39 cells in fifteen cell culture dishes (150 mm, inner diameter) were harvested by scraping and pelleted by centrifugation ($200 \times g$ for 5 min at 4°C). After being washed with PBS three times, each cell pellet was resuspended in 10 mM Tris-HCl buffer, pH 7.5, containing 0.25 M sucrose and Complete™, EDTA-free (Roche, Mannheim, Germany) to achieve a final volume equal to five times the volume of the cell pellet (*i.e.* a 20% cell suspension). The cell suspension was homogenized with a ball-bearing homogenizer (*48*), and then centrifuged at $800 \times g$ for 5 min at 4°C. One milliliter of each post-nuclear supernatant fraction was layered under 2 ml of 10 mM Tris-HCl buffer, pH 7.5, containing 0.15 M NaCl (TN-buffer). After centrifugation at $100,000 \times g$ for 60 min at 4°C, the lipid droplet fraction, *i.e.* the distinct white band on the top of the preparation, was collected with a pipetman. The floating lipid droplet fraction was diluted with 3.5 ml of TN-buffer and then re-purified by centrifugation ($100,000 \times g$ for 30 min at 4°C). This washing step was repeated three times. Lipid droplets in the floating fractions in both cells were enriched up to more than 500-fold compared with those in the total cell lysates as estimated by their protein contents. The amounts of lipid droplets isolated from Hepswx and Hep39 cells were nearly the same. The purified lipid droplet fractions (~0.1 mg of protein per ml) were stored at −80°C until use. The purity of the lipid droplet fractions was verified by microscopic and immunoblot (Fig. 1) analyses. Adipose differentiation–related protein (ADRP), a known lipid droplet protein, was significantly enriched in the lipid droplet fractions of Hepswx and Hep39 cells (Fig. 1). Other organelle marker proteins, such as nucleoporin p62 for the nucleus, prohibitin for the mitochondria, fatty acid synthase for the cytoplasm, GM130 for the Golgi apparatus, EEA1 for the early endosome, or annexin II for the plasma membrane, were not detected in the lipid droplet fractions of either cells (Fig. 1). Small amounts of calnexin, a marker of the endoplasmic reticulum, which is a major organelle, were detected in the lipid droplet fractions of both cells to a similar extent. Although we did not detect calnexin in the lipid droplet fractions by proteomic analysis (see Tables 1 and 2), the lipid droplet fractions of both cells could be contaminated with a small amount of endoplasmic reticulum.

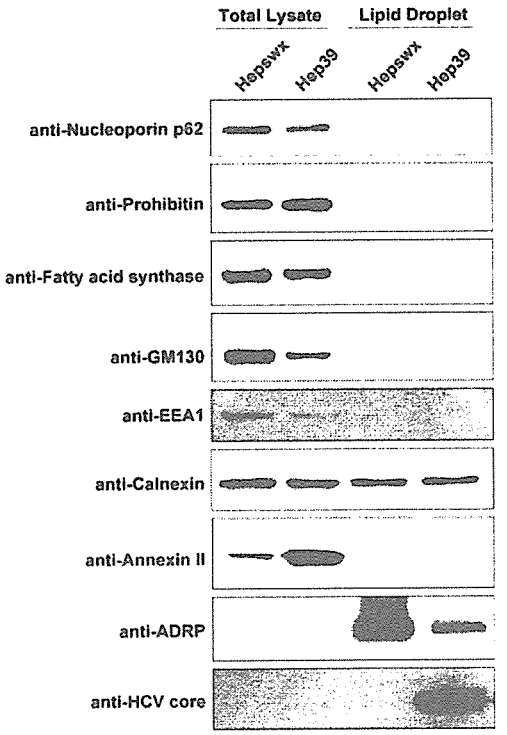

Fig. 1. **Immunoblot analysis of lipid droplet fractions in Hepswx and Hep39 cells using antibodies against various organelle markers.** Total cell lysates and lipid droplet fractions (1.5 μg of protein per lane in the case of anti-ADRP; 5 μg of protein per lane in others) from Hepswx and Hep39 cells were analyzed by immunoblotting with the indicated antibodies.

1-D-SDS-PAGE/MALDI-TOF MS Analysis—The lipid droplet fraction (30 μg protein) of each cell line was fractionated in a 10% SDS–polyacrylamide gel, and the gel was stained with Coomassie Brilliant Blue. The protein bands were excised from the gel and subjected to in-gel trypsin digestion. The tryptic peptide mixtures were analyzed by MALDI-TOF MS as described previously (*49*). Prior to MALDI-TOF MS analysis, the peptide mixtures were desalted using C18 Zip Tips (Millipore, Billerica, MA, USA) according to the manufacturer's instructions. The peptide data were collected in the reflection mode and with positive polarity, using a saturated solution of

Table 1. **Lipid droplet proteins identified in Hepswx and Hep39 cells by means of 1-D-SDS-PAGE/MALDI-TOF MS.**

Protein	Molecular mass (kDa) (calc.)	Accession No.	SDS band No.[a]	
			Hepswx	Hep39
PAT family proteins				
Adipose differentiation–related protein (ADRP)	48.1	34577059	5	21
Cargo selection protein/TIP47	47.0	20127486		22
Lipid metabolism				
Acyl CoA synthetase long chain family member 3	80.4	42794752	4	18
Cytochrome b_5 reductase	34.3	4503327	9	26
Lanosterol synthase	83.3	4808278	4	18
NAD(P)-dependent steroid dehydrogenase-like; H105e3	41.9	8393516	8	25
Retinal short-chain dehydrogenase/reductase retSDR2	33.0	7705905	10	27
Cytosolic phospholipase A_2	85.2	1352707		14
Rab GTPases				
Rab1A	22.7	4758988	13	30
Rab1B	22.2	23396834	13	30
Rab5C	23.5	38258923	11	28
Rab7	23.5	34147513	12	29
RNA metabolism/binding				
DEAD box protein 1 (DDX1)	82.9	6919862		16
DEAD box protein 3 (DDX3)	73.2	3023628		18
HC56/gemin 4	118.8	10945430		15
Other/unknown proteins				
BiP protein	70.9	14916999	3	17
CGI-49 protein	46.9	7705767	6	23
Heat shock protein gp96 precursor	90.2	15010550	2	14
Ancient ubiquitous protein 1	41.4	31712024	7	
Major vault protein	99.3	15990478	1	
Apoptosis-inducing factor–homologous mitochondrion-associated inducer of death	40.5	13543964		24
KIAA0887 protein	52.4	4240263		21
Protein disulfide-isomerase [EC 5.3.4.1] ER60 precursor	56.7	1085373		20
Transport-secretion protein 2.1	57.7	9663151		19
HCV core protein	20.6	974345		31

[a]Band numbers correspond to those in Fig. 2.

α-cyano-4-hydroxycinnamic acid (Sigma) in 50% acetonitrile and 0.1% trifluoroacetic acid as the matrix. Spectra were obtained using a Voyager DE-STR MALDI-TOF mass spectrometer (PE Biosystems, Foster City, CA, USA). Internal calibration was performed with adrenocorticotropic hormone, fragment 18–39 (Sigma), and bradykinin fragment (Sigma). The data base–fitting program MS-Fit available at the WWW site of the University of California, San Francisco (prospector.ucsf.edu/ucsfhtml3.4/msfit.htm) was used to interpret the MS spectra of protein digests (*50*).

DNLC-MS/MS Analysis—The lipid droplet fraction (10 μg protein) of each cell line was first delipidated by chloroform–methanol extraction as originally described (*51*). Two volumes of chloroform and 1 volume of methanol were mixed with 0.8 volume of the lipid droplet fraction. Then, 1 volume of chloroform and 1 volume of water were added to the mixture, and the mixture was vortexed for 30 s, and centrifuged at 10,000 × *g* for 5 min at room temperature. The resulting organic (lower) phase was removed. The aqueous (upper) phase and interface, containing all the lipid droplet proteins, was lyophilized. The delipidated lipid droplet proteins were digested with endoproteinase Lys-C, and the resulting peptides were analyzed by DNLC-MS/MS as described (*52*, *53*).

Cell Fractionation—All manipulations were performed at 4°C or on ice. After being washed with PBS, confluent monolayers of Hepswx and Hep39 cells were harvested by scraping and pelleted by centrifugation (200 × *g*, 5 min). The precipitated cells were homogenized with a ball-bearing homogenizer in 10 mM Tris-HCl buffer, pH 7.5, containing 0.25 M sucrose, and Complete™, EDTA-free. After centrifugation of the lysate at 800 × *g* for 5 min, the cytosolic fraction (100,000 × *g* supernatant) and membrane fraction (100,000 × *g* precipitate) were separated from the post-nuclear supernatant fraction by centrifugation at 100,000 × *g* for 60 min. The membrane fraction was resuspended in TN-buffer and then re-purified twice by centrifugation. The protein concentrations of these preparations were determined with BCA protein assay reagents (Pierce Biotechnology, Rockford, IL, USA) using BSA as a standard.

Immunoblot Analysis—Equivalent amounts of proteins from Hepswx and Hep39 cells were separated in a 10 or 12.5% SDS–polyacrylamide gel and then electrophoretically transferred to a polyvinylidene difluoride membrane. The membranes were blocked overnight at 4°C or 30 min at room temperature in TBS containing 0.1% Tween 20 and 5% skim milk. The blots were probed with a mouse

Table 2. **Lipid droplet proteins identified in Hepswx and Hep39 cells by means of DNLC-MS/MS.**

Protein	Accession No.	Molecular mass (kDa) (calc.)	Matched peptide sequence	
			Hepswx[a]	Hep39[a]
PAT family proteins				
Adipose differentiation–related protein (ADRP)	34577059	48.1	+ TITSVAMTSALPIIQK DAVTTTVTGAK EVSDSLLTSSK	+ TITSVAMTSALPIIQK DAVTTTVTGAK EVSDSLLTSSK
Cargo selection protein / TIP47	20127486	47.0	+ VSGAQEMVSSAK	+ VSGAQEMVSSAK
Lipid metabolism				
Acyl-CoA synthetase long-chain family member 3	42794752	80.4	+ VLSEAAISASLEK	+ ELTELARK
Cytochrome b_5 reductase	4503327	34.2	+ DILLRPELEELRNK	+ SNPIIRTVK
Gastric-associated differentially-expressed protein YA61P	6970062	14.9	+ AIGLVVPSLTGK	+ AIGLVVPSLTGK
Retinal short-chain dehydrogenase/ reductase retSDR2	7705905	33.0	+ HGLEETAAK	+ FDAVIGYK
Sterol carrier protein 2–related form, 58.85K	86717	58.8	+ LQNLQLQPGNAK	+ LQNLQLQPGNAK
Acyl-CoA synthetase long-chain family member 4	4758332	74.4	+ SDQSYVISFVVPNQK	
Fatty acid binding protein 5	4557581	15.2	+ ELGVGIALRK	
Hydroxysteroid (17-beta) dehydrogenase 4	4504505	79.7		+ NHPMTPEAVK
Rab GTPases				
Rab1A	4758988	22.6	+[b] QWLQEIDRYASENVNK RMGPGATAGGAEK	+ RMGPGATAGGAEK
Rab1B	23396834	22.1	+[b] QWLQEIDRYASENVNK	+ RMGPGAASGGERPNLK
Rab7	34147513	23.5	+ NNIPYFETSAK	+ ATIGADFLTK
Rab18	20809384	22.9	+ HSMLFIEASAK	+ ILIIGESGVGK
Rab10	12654157	22.5	+ LLLIGDSGVGK	
Rab11	4758986	24.5	+ VVLIGDSGVGK	
Rab8	539607	23.6		+ IRTIELDGK
RNA metabolism/binding				
DEAD box protein 1 (DDX1)	6919862	82.4		+ FGFGFGGTGK
DEAD box protein 3 (DDX3)	3023628	73.2		+ GVRHTMMFSATFPK
IGF-II mRNA-binding protein 3	30795212	63.7		+ EGATIRNITK
Ribosomal protein L29	14286258	17.8		+ AQAAAPASVPAQAPK
Other/unknown proteins				
Apoptosis-inducing factor homologous mitochondrion-associated inducer of death	13543964	40.5	+ EVTLIHSQVALADK	+ EVTLIHSQVALADK
BiP protein	14916999	72.3	+ SQIFSTASDNQPTVTIK	+ VYEGERPLTK
Hypothetical protein DKFZp586A0522.1	7512845	28.2	+ LQHIQAPLSWELVRPH-IYGYAVK	+ RELFSNLQEFAGPSGK
Prolyl 4-hydroxylase, beta subunit	20070125	57.1	+ VHSFPTLK	+ AEGSEIRLAK
Ancient ubiquitous protein 1	31712024	41.4	+ GTQSLPTASASK	
Heat shock protein gp96 precursor	15010550	90.2	+ FAFQAEVNRMMK	
Hypothetical protein FLJ21820	11345458	37.3	+ DIYGLNGQIEHK	
Molecule possessing ankyrin repeats induced by lipopolysaccharide	38173790	78.1	+ CLIQMGAAVEAK	
Ubiquitin-conjugating enzyme E2G 2, isoform 1	15079469	18.6	+ RLMAEYK	
CGI-49 protein	7705767	46.9		+ AGGVFTPGAAFSK
DILV594	37182139	31.4		+ RELFSQIK
Hypothetical protein DKFZp564F0522.1—human (fragment)	7512734	33.1		+ ILRTSSGSIREK
Hypothetical protein HSPC117	7657015	55.2		+ EQLAQAMFDHIPVGVGSK
Tumor protein D52–like 2 isoform e	40805860	22.2		+ TQETLSQAGQK
Vesicle amine transport protein 1	15679945	41.9		+ VVTYGMANLLTGPK

[a]+, detected. [b]This peptide sequence is present in both Rab1A and Rab1B.

monoclonal anti-ADRP antibody (PROGEN Biotechnik GmbH, Heidelberg, Germany) (1:25), a guinea pig polyclonal anti-TIP47 antibody (PROGEN Biotechnik GmbH) (1:250), a mouse monoclonal anti-HCV core protein antibody (Anogen, Ontario, Canada) (1: 1,000), a mouse monoclonal anti-DDX1 antibody (Pharmingen, San Diego, CA, USA) (1:500), or a rabbit polyclonal anti-DDX3 antibody (antibody custom-made by Invitrogen, CA, USA) (1:500) for 90 min at room temperature. The blots were then incubated with horseradish peroxidase (HRP)–conjugated goat anti-rabbit IgG (BIO-RAD), HRP-conjugated goat anti-mouse IgG (BIO-RAD), or HRP-conjugated goat anti-guinea pig IgG (ICN Pharmaceuticals, Aurora, OH, USA) at 1:2,000 dilution for 60 min. Detection of immunoreactive proteins was performed with an ECL system (Amersham Biosciences Corp., Piscataway, NJ, USA).

RESULTS

Proteomic Analysis of Lipid Droplets by 1-D-SDS-PAGE/MALDI-TOF MS—Lipid droplet proteins from control (HCV core non-expressing) Hepswx cells and HCV core–expressing Hep39 cells were separated by 10% SDS-PAGE, and the protein bands were visualized by Coomassie Brilliant Blue staining (Fig. 2). In each cell line ~30 bands were seen. The visible bands (areas) were excised from the gels, trypsinized, and analyzed by MALDI-TOF MS. Among the 31 bands, we identified 25 proteins: 15 proteins in Hepswx cells and 23 proteins in Hep39 cells (Fig. 2 and Table 1). Thirteen of the 25 proteins were detected in both types of cell. The lipid droplet proteins found in both Hepswx and Hep39 cells could be categorized into four groups: (1) PAT family proteins, *i.e.* ADRP and TIP47; (2) multiple molecules involved in lipid metabolism; (3) several Rab GTPases; and (4) other/unknown proteins (Table 1). In addition, Hep39 cells contained another group of proteins involved in RNA metabolism/binding (Table 1).

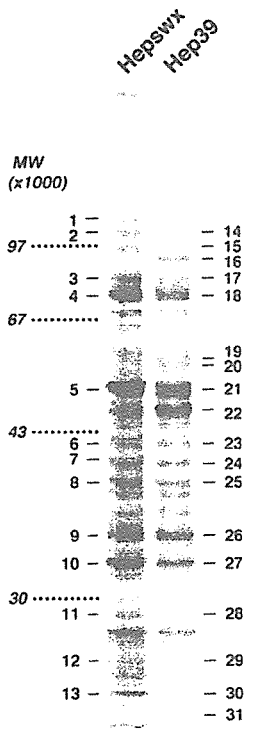

Fig. 2. **Signature SDS-PAGE patterns of the lipid droplet fractions of Hepswx and Hep39 cells.** Proteins in the purified lipid droplet fractions (30 μg of protein per lane) of Hepswx cells and Hep39 cells were separated in a 10% SDS–polyacrylamide gel, and visualized by Coomassie Brilliant Blue staining. The 31 numbered bands were excised from the gel, subjected to in-gel trypsin digestion, and processed for MALDI-TOF-MS. Molecular weights (MW) are given to the left of the gel.

Proteomic Analysis of Lipid Droplets by DNLC-MS/MS—Some protein bands in Fig. 2 could not be identified, probably due to the restricted separation capacity of 1-D-SDS-PAGE (*i.e.* multiple proteins migrating to the same area). We had, however, difficulty in applying 2-DE to the separation of lipid droplet proteins because of their hydrophobic characteristics. We then tried a new LC-based MS strategy. Lipid droplet fractions from Hepswx and Hep39 cells were delipidated and then digested with Lys-C. The resulting peptide mixtures were directly analyzed using a DNLC-MS/MS system (*52*). We identified 36 lipid droplet proteins: 24 proteins in Hepswx cells and 27 proteins in Hep39 cells (Table 2). Twenty-three lipid droplet proteins were newly identified with this system. Fifteen proteins detected in both cell lines were classified into four categories (Table 2) as in the case of 1-D-SDS-PAGE/MALDI-TOF MS analysis. A group of proteins involved in RNA metabolism/binding was also found only in Hep39 cells (Table 2).

Proteins Exhibiting Differences in Their Association with Lipid Droplets Due to HCV Core Protein Expression—SDS-PAGE patterns of lipid droplet proteins were similar but revealed several distinct differences in protein composition between Hepswx and Hep39 cells (Fig. 2). The most remarkable differences were seen in the bands corresponding to PAT family proteins. The amount of ADRP, a major PAT family protein in lipid droplets in the liver (*54*, *55*), and likely to be the most abundant lipid droplet protein in Hepswx cells (Fig. 2, band 5), seemed to be less in HCV core–expressing Hep39 cells (Fig. 2, band 21). On the other hand, TIP47, which is also known to be a PAT family protein in lipid droplets (*56*, *57*), was detected as a major protein only in Hep39 cells (Fig. 2, band 22, and Table 1). To confirm these findings, the contents of ADRP and TIP47 in the lipid droplet fractions of Hepswx and Hep39 cells were examined by immunoblot analysis with specific antibodies. The lipid droplet fraction of HCV core–expressing Hep39 cells showed an apparently lower content of ADRP and a much higher content of TIP47 than the levels in Hepswx cells (Fig. 3).

Next we examined the cellular distributions of ADRP and TIP47 in Hepswx and Hep39 cells by cell fractionation. ADRP was highly concentrated in the lipid droplet fractions of both cells, even though the content in the lipid droplets was much lower in Hep39 cells than in Hepswx cells (Fig. 4). ADRP was not detected in post-nuclear supernatant fractions or in either the cytosol or membrane fractions, probably because of low expression levels in these cells or low affinity of the anti-ADRP antibody we used

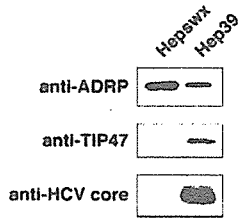

Fig. 3. **The lipid droplet fraction of Hep39 cells contains less ADRP, but more TIP47, than Hepswx cells.** Lipid droplet fractions (1.5 μg of protein per lane) from Hepswx and Hep39 cells were analyzed by immunoblotting with the indicated antibodies.

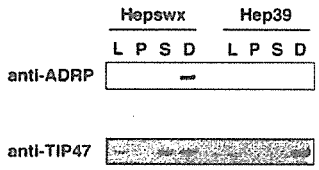

Fig. 4. **Subcellular localization of ADRP and TIP47 in Hepswx and Hep39 cells.** Hepswx and Hep39 cells were fractionated into post-nuclear supernatant (lane L), 100,000 × *g* precipitate (lane P), 100,000 × *g* supernatant (lane S), and lipid droplet (lane D) fractions as described in "MATERIALS AND METHODS." Ten micrograms of protein was processed for gel electrophoresis, and then analyzed by immuonoblotting with anti-ADRP and anti-TIP47 antibodies.

(Fig. 4). The mRNA expression level of ADRP in Hep39 cells was less than half that in Hepswx cells (data not shown), consistent with the immunoblot data shown in Fig. 4. These results suggest that the lower ADRP content in the lipid droplet fraction of Hep39 cells is due to a low expression level of ADRP. In contrast, Hep39 cells had much more TIP47 in the lipid droplet fraction (Figs. 3 and 4, lanes D), but the cellular TIP47 content of Hep39 cells was not more than that in Hepswx cells (Fig. 4, lanes L). Besides the lipid droplet fraction, the cytosolic fraction of Hepswx cells was found to contain TIP47 at a substantial level, while the cytosolic fraction of Hep39 cells did not (Fig. 4, lanes S). These results indicate that the intracellular distribution of TIP47 shifts drastically from the cytosol to lipid droplets in HCV core–expressing Hep39 cells.

Another obvious difference between Hepswx and Hep39 cells in Fig. 2 is the presence of a specific ~85 kDa band (Fig. 2, band 16) in Hep39 cells, which was identified as DEAD box protein 1 (DDX1), a DEAD box protein family member, by 1-D-SDS-PAGE/MALDI-TOF MS analysis (Table 1). DNLC-MS/MS analysis also supported the existence of DDX1 in the lipid droplet fraction of Hep39 cells (Table 2). In addition, DEAD box protein 3 (DDX3), another DEAD box protein family member, was also detected in the lipid droplet fraction of Hep39 cells by means of the two different strategies used for proteomic analysis (Tables 1 and 2), suggesting that DDX3 is a major lipid droplet protein in Hep39 cells. To verify the association of DDX 1 and DDX3 with lipid droplets in Hep39 cells, immunoblot analysis was carried out. Figure 5 shows that DDX 1 and DDX 3 exist in the lipid droplet fraction of HCV core-expressing Hep39 cells, but not Hepswx cells. These results imply the

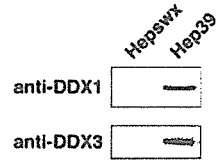

Fig. 5. **Hep39 cells, but not Hepswx cells, have DDX1 and DDX3 in the lipid droplet fraction.** Lipid droplet fractions (0.5 μg of protein per lane) in Hepswx and Hep39 cells were analyzed by immunoblotting with anti-DDX1 and anti-DDX3 antibodies.

special pathological functions of DDX1 and DDX3 in lipid droplets in HCV core–expressing cells.

DISCUSSION

To analyze lipid droplet proteins, we performed proteomic analysis by means of 1-D-SDS-PAGE/MALDI-TOF MS and automated DNLC-MS/MS, and identified 25 and 36 proteins, respectively (Tables 1 and 2). Many more lipid droplet proteins were identified by DNLC-MS/MS, and 22 major proteins separated by 1-D-SDS-PAGE (Fig. 2, bands, 2, 3, 4, 5, 7, 9, 10, 12, 13, 16, 17, 18, 21, 22, 24, 26, 27, 29, and 30) and detected on MALDI-TOF MS analysis were also detected on DNLC-MS/MS analysis. These results indicate that DNLC-MS/MS is a very sensitive and reliable system as well as a high-throughput method. Particularly, DNLC-MS/MS would be a powerful system for exhaustive proteomic analysis of protein mixtures/complexes (up to ~100 proteins) such as lipid droplets.

In our targeted proteomic study, we identified a total of 48 lipid droplet proteins: 30 proteins in control Hepswx cells, 38 proteins in HCV core–expressing Hep39 cells, and 20 proteins in both cell lines. The resident lipid droplet proteins were classified into four groups (Tables 1 and 2), consistent with the recently reported data obtained on proteomic analysis of lipid droplet proteins in other cell lines (*58–60*). In addition, multiple proteins, such as the sterol carrier protein 2–related form, fatty acid binding protein 5, and apoptosis-inducing factor homologous mitochondrion-associated inducer of death, were newly identified as lipid droplet proteins in this study. These accumulated data obtained on proteomic analysis will be useful for understanding the biogenesis and functions of lipid droplets about which little is yet known.

A prominent effect of the expression of HCV core protein on the composition of lipid droplet proteins was observed among the PAT family proteins, i.e. ADRP and TIP47. HCV core–expressing Hep39 cells contained much less ADRP in the lipid droplet fraction (Fig. 3), probably because of the lower cellular expression level and the lack of induction of expression upon lipid loading (data not shown). In contrast, a substantial amount of TIP47 was associated with the lipid droplet fraction of Hep39 cells (Fig. 3). Perilipin, a structural protein of lipid droplets in adipocytes, ADRP, and TIP47, termed PAT family proteins (*61*), share extensive amino acid sequence similarity (*61–63*), suggesting a common biological function in lipid droplet formation. For example, the transition in surface protein composition of lipid droplets from ADRP to perilipin occurs during adipocyte differentiation (*64*). Thus, TIP47 might replace ADRP